



HAL
open science

Furniture wood waste depollution through hydrolysis under pressurized water steam: Experimental work and kinetic modelization

Maximilien Gibier, Mohammad Sadeghisadeghabad, Pierre Girods, André Zoulalian, Yann Rogaume

► To cite this version:

Maximilien Gibier, Mohammad Sadeghisadeghabad, Pierre Girods, André Zoulalian, Yann Rogaume. Furniture wood waste depollution through hydrolysis under pressurized water steam: Experimental work and kinetic modelization. *Journal of Hazardous Materials*, 2022, 436, pp.129126. <10.1016/j.jhazmat.2022.129126>. <hal-03715637>

HAL Id: hal-03715637

<https://hal.science/hal-03715637v1>

Submitted on 22 Jul 2024

HAL is a multi-disciplinary open access archive for the deposit and dissemination of scientific research documents, whether they are published or not. The documents may come from teaching and research institutions in France or abroad, or from public or private research centers.

L'archive ouverte pluridisciplinaire HAL, est destinée au dépôt et à la diffusion de documents scientifiques de niveau recherche, publiés ou non, émanant des établissements d'enseignement et de recherche français ou étrangers, des laboratoires publics ou privés.



Distributed under a Creative Commons CC BY-NC 4.0 - Attribution - Non-commercial use - International License

1 Title: Furniture wood waste depollution through hydrolysis under pressurized water steam:
2 Experimental work and kinetic modelization

3 Maximilien GIBIER, Mohammad SADEGHISADEGHABAD, Pierre GIRODS, André ZOULALIAN, Yann
4 ROGAUME.

5 Université de Lorraine, INRAE, LERMAB, ERBE, F - 88 000 EPINAL, France

6

7

8 Abstract:

9 As the Recycling of wood waste becomes more important each year, wood products that contain
10 urea-formaldehyde resins gained more attention due to the release of formaldehyde and other
11 chemicals which have a critical impact on humans health and the environment. In this study, the
12 hydrolysis of wood wastes from a French furniture industry was studied under different controlled
13 conditions (temperature/pressure, steam ratio). An original on-line method to measure the emission
14 of formaldehyde and ammonia using a FTIR spectrometer and a dilution system was applied
15 successfully in this study. The effect of operatory conditions on formaldehyde and ammonia released
16 is discussed. A mathematical model was also introduced to model the behavior of the ammonia and
17 formaldehyde emission in the hydrolysis of wood waste.

18 **Keywords:**

19 Wood waste remediation, Urea-formaldehyde resin, hydrolysis, FTIR on-line measurement, Kinetic
20 modelisation

21

22 Environmental Implication:

23 This paper is focused on the hydrolysis process used to remove pollutants from wood waste, namely
24 from the furniture sector. Such waste contains high quantities of resins, namely urea-formaldehyde
25 resins which contains nitrogen and are responsible for Nox emissions during its valorization by
26 combustion or of formaldehyde and ammonia if the landfilling is preferred. This work aim therefore
27 to develop a depollution process using no chemical reagent and being as energy efficient as possible
28 to favor the use of end-life wood as raw material for different industrial sectors such as wood panel
29 boards (Insulation panels, MDF, particleboard, ...).

30 1. Introduction

31

32 Renewable energy is undoubtedly the most suitable approach to the challenges caused by fossil
33 fuels. As a significant part of the biomass, wood is the focus of many studies. Wood has several
34 advantages regarding the bio-economy concept. Wood as a natural material offers many outstanding
35 characteristics in thermal conductivity and mechanical strength, which expands its use into many
36 areas. Its consumption has increased from the beginning of the last century for different new
37 applications (Bernstein et al., 2016) such as energy production, building materials, chemicals, etc. At
38 the same time, wood waste consumption from end-of-life wood-based products is increasing. Wood
39 waste contains additives and pollutants (resins, paints, preservatives, heavy metals, etc.) and
40 contaminating materials (metals, plastics, glass, stocks, etc.), making recycling wood waste much
41 more complicated than raw wood (Besserer et al., 2021).

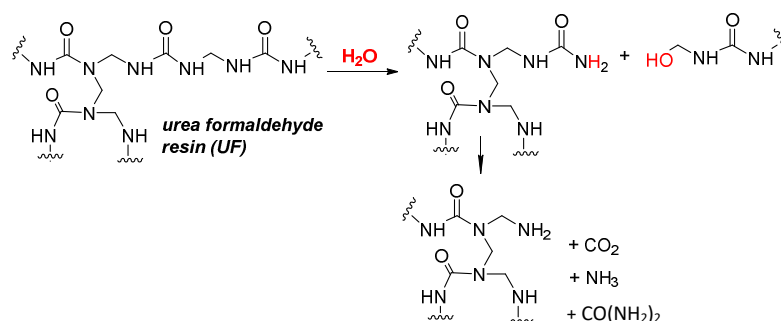
42 Wood waste-based matters from products at their end-life show a notable amount of material to be
43 valued in agreement with EC Waste Directive 2008/98. The construction, destruction, and aged
44 furniture waste that holds many wood-based agglomerates, are the main waste streams in the
45 European Union (Ihnát et al., 2017). In France in 2018, the furniture industry as a great source of
46 agglomerated wood waste materials such as particleboards (PBs), produced almost 2 million tons of
47 pieces of furniture which half ended up landfilled (Waste furniture sector France report, 2020).
48 Today, the wood waste management strategy is mainly based on disposal (landfill and incineration),
49 energy recovery, and material recovery (Lykidis and Grigoriou, 2008).

50 Even if the material recovery way is much more complicated than others, it appears to be the best
51 way for various reasons; it allows extending carbon storage in matters, which could slow down its
52 release in CO₂ form at end-life energy recovery (Lubke et al., 2020). This large amount of material
53 could also constitute an abundant and inexpensive source of raw matter for new materials
54 production while limiting economic stress on the wood industrial field caused by increased wood
55 consumption (Besserer et al., 2021).

56 The main contaminant of furniture waste wood, especially PBs and MDF (medium density
57 fiberboard), is the resin used as glue. The most common resin is urea-formaldehyde (UF) resin (Irle et
58 al., 2010). Indeed, UF glue presents many advantages with a low cost, a high chemical reactivity
59 (short polymerization duration), and an absence of color after polymerization (Liu et al., 2018; Irle et
60 al., 2010). Unlike other waste wood contaminants (plastics, metals, glass) which could be sorted
61 automatically, adjuvants like resin could not be easily eliminated (Ren et al., 2022). It is therefore
62 essential to find a way to “clean up” such a waste before using it as new raw material for recycling.

63 Two ways have been identified to remove UF resin from wood waste. The first one is the pyrolysis
64 process conducted in low severity conditions (between 250 and 300°C for some minutes). In different
65 studies, it was shown that low-temperature pyrolysis (<350°C) could remove up to 70% of the
66 nitrogen in PBs (Girods, 2008; Girods et al., 2008, 2009a, 2009b), in which the nitrogen content was
67 used as resin content indicator knowing that natural nitrogen content in wood is very low (<0.1%)
68 (Cowling and Merrill, 1966). Low-temperature pyrolysis mixed with combustion was also suggested
69 (Jiang et al., 2010). This approach could be insufficient since ammonia might still be converted to
70 nitrogen oxides during the combustion step in oxygen-rich circumstances.

71 The second way identified is based on one of the weaknesses of UF resin, namely its sensibility to
72 water which limits, therefore, its use in outdoor applications (Irle et al., 2010). It is known that the
73 presence of moisture can make the UF polymer chain go through a hydrolysis reaction (i.e., the
74 chemical mechanism described in Fig. 1) which leads to shorter polymer pieces and aggravates the
75 mechanical properties of the wood-UF composite (Besserer et al., 2021).



86 Figure 1. Prolysis of urea—formaldehyde resin (adapted from Hagel and Saake, 2020)

87

88 The susceptibility of UF-based adhesives to hydrolysis can be used in favor of recycling wood-based
89 PBs that use these adhesives as glue in their structure.

90 The condensation and hydrolysis reactions of UF resin are largely described in the literature
91 (Samaržija-Jovanović et al., 2011; Myers, 1986; Myers, 1982; Pizzi and Mittal, 2003). The hydrolysis
92 reaction of UF resin leads mainly to forming formaldehyde, urea and intermediate compounds (resin
93 fragments) of various molecular weights (Lubis et al., 2018). According to Myers and Koutsky (1990),
94 the hydrolysis of all the bonds of the UF resin leads to the release of formaldehyde, with the
95 exception of the C=O carbonyl and C-N amide bond. The works of Wan et al. (2014) and Hagel et al.
96 (2020) showed an increase in pH is linked to the presence of ammonium ions in the water, which
97 suggests the production of ammonia following the hydrolysis of the UF resin polymers.
98 Steam cooking can be used to separate the UF resin from the wood fibers in wood wastes by
99 hydrolysis in a pressurized saturated steam environment (Lubis et al., 2018). It has been shown that
100 the hydrolysis of cured resins is strongly affected by the pH of the medium in the following order acid
101 > neutral > alkali. The optimum conditions to eliminate UF resin from MDF were found to be 80°C for
102 2 hours in the presence of oxalic acid (Lubis et al., 2018). Compared to acidic conditions, pure steam
103 treatments are less expensive due to the use of less corrosive materials, and there is no need for a
104 separation step, which makes the process more environmentally friendly (Hagel et al., 2020).
105 Another study also showed that this hydrolysis reaction could be facilitated by treatment at higher
106 temperatures using water steam. In the study, water steam at temperatures of 150–190°C for 10–20
107 minutes removed almost 80% of the resins (Wan et al., 2014). Different approaches have been tried
108 to approximate the stability of UF resins facing hydrolysis by testing the formaldehyde release and
109 structural stability (Park et al., 2013; Ringena et al., 2006).

110 Among all the information, it could be stated that literature is rich concerning the hydrolysis process
111 used to “clean up” wood waste contaminated by UF resin. In literature, studies on this concept have
112 been performed mainly in the liquid phase, using chemical agents. In addition, no possible on-line
113 monitoring of the depollution of UF has been proposed. To our knowledge, no articles deal with
114 neither the on-line measurement of emissions during the hydrolysis nor the kinetics of such a curing
115 process.

116 It is therefore proposed in this work to investigate hydrolysis as an efficient method for the
117 depollution of wood waste under steam pressure at lab scale in batch mode. The effect of the couple
118 pressure/temperature and the steam ratio on the efficiency and the kinetics of the reaction has been
119 studied. Gas emissions are on-line measured through FTIR spectrometer analysis to follow in real-
120 time the decomposition products of UF resin. HPLC measurements on liquids and Kjeldahl on solid
121 phases are performed to confirm FTIR measurements. Finally, a kinetic model based on a simplified
122 chemical mechanism is proposed to allow the prediction of gas emissions according to steam curing
123 operatory conditions. This last point is essential to supply reliable information for scaling such a
124 process at the industrial scale.

125
126

127 2. Materials and methods

128 2.1 Wood wastes

129 The crushed wood waste was supplied by VALDELIA (A French eco-organism that ensures the
130 collection of professional waste furniture). The waste is crushed by their sorting center, allowing a
131 relatively homogeneous mixture. The particle size of the wood waste supplied ranges from 0 to
132 30 mm. After the reception, the wood waste is first sorted using a mechanical sieve, equipped with a
133 1cm×1cm sieve in order to remove fine particles as well as metal pieces manually.

134 The composition of the waste batch used in our study (about 4m³) is evaluated on the content of 2kg
135 of wood waste: 42% of raw wood, 51% of particleboard and 7% of fiberboard. No MDF was identified
136 in this batch of wood waste.

137 It was decided to choose actual waste coming from landfill and not from new panels in order to
138 simulate properly the use of waste. Indeed, their storage in landfill (wet and outdoor conditions,
139 micro-organisms) can lead to the beginning of glues degradation (Lee et al., 2014). The proportion of
140 waste contaminated by melamine-formaldehyde and phenol-formaldehyde resins is therefore
141 unknown. The nitrogen content on a dry basis was measured at 2.5%.

142 Wood waste was dried in stainless steel bins in an oven at 103°C for 7 days before the steam cooking
143 experiments to get rid of unstability of moisture of waste with time and to assume a better control of
144 the inlet waste sample mass. Moisture content after the drying step was assumed to be inferior to
145 2%.

146

147 2.2 Kjeldahl analysis

148

149 Kjeldahl analysis is a relatively simple method for determining nitrogen of various nitrogen
150 compounds such as amines and quaternary ammonium salts. It does not allow the direct dosage of
151 nitrates, nitrites, nitrosyls, and cyanides, which must first be reduced to ammonia (Hepburn, 1908).
152 The Kjeldahl method was performed in three steps of mineralization, distillation, and titration
153 (Hepburn, 1908). The mineralization process was performed in a BUCHI Speed Digester K-436.
154 Titration was afterward performed using a digital pH meter (Titroline easy, Schott, Mainz, Germany).

155 Kjeldahl was used to evaluate the mass of nitrogen removed by comparing the mass of nitrogen in
156 the solid sample before and after the experiment. Assuming that the mass loss of waste is negligible
157 during the test (loss of mass not determinable on the device), the mass of nitrogen removed can
158 then be calculated.

159 2.3 HPLC method

160

161 High-Performance Liquid Chromatography (HPLC) was used to quantify the formaldehyde in liquid
162 samples, a well-known method available in the literature (Ihnát et al., 2017; Li et al., 2007; Nishikawa
163 and Sakai, 1995; Wahed et al., 2016; Xu et al., 2011). The HPLC measurement was performed on a
164 ThermoFischer UltiMate 3000, equipped with an Acquity UPLC BEH C18 column, with a particle size
165 of 1.7 µm (50mm x 2.1mm id.). Separation was achieved using a mixture of water/acetonitrile (60:40,
166 v/v between 0-4 min - 10:90, v/v between 4-6min - 60:40, v/v between 6-10min). The total run time
167 was 10 min. The flow rate was 0.3 mL/min and the injection volume was 1 µL.

168 The formaldehyde contained in the sample requires a derivatization step to be quantified by HPLC.
169 The pH of the sample is first adjusted to 5. 1 mL of solution is taken and centrifuged for 10 min at
170 12,000 rpm. The sample is then filtered with a syringe and a 45µm diameter nylon filter. 20 µL of the
171 sample was placed in a 1.5 ml glass vial with 30µL of DNPH solution (derivatization reagent) and 1 mL
172 of acetonitrile (disperser). The sample was mixed using a Vortex-mixer and stored for HPLC analysis.
173 The HPLC software automatically calculates the amount of formaldehyde measured in the sample by
174 comparing the area obtained with the area of a 2µg/ml standard solution.

175

176 2.4 FTIR measurements

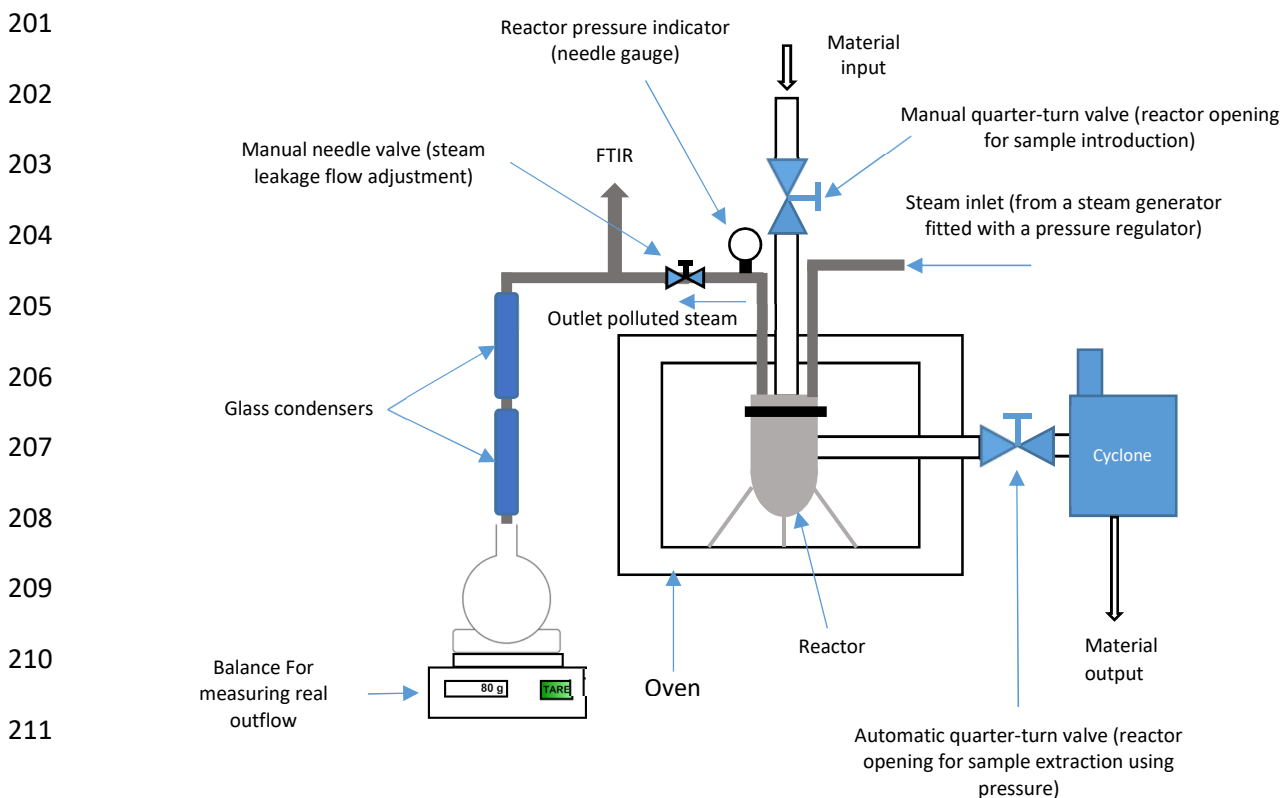
177
178 HPLC and Kjeldahl methods determine depollution process efficiency, but they are off-line and
179 quantitative analysis. That is why an on-line qualitative and quantitative measurement method has
180 been developed to characterize hydrolysis products of wood waste and follow the kinetic of
181 pollutants devolatilization. Infrared spectrometry has been chosen for these analyzes since it allows
182 fast, qualitative and quantitative analysis of the gas phase. Since gas effluents of the hydrolysis
183 process mainly consist of water steam (more than 99 vol.%) and because of a high sensibility and a
184 large adsorption band of water with Infrared spectrometry, a dilution system (dilution in nitrogen
185 with a ratio close to 100x) has been added.

186 The infrared spectrometer (FTIR) used was a GASMET DX-4000 FTIR multi-component gas analyzer
187 (Temet Instruments OY, Finland), a portable FTIR gas analyzer. The resolution of the obtained spectra
188 was 8 cm^{-1} . The device was used to measure the ammonia and formaldehyde emissions during
189 hydrolysis. The calibration of the FTIR spectrometer was obtained on pure water steam after dilution
190 in nitrogen.

191 Formaldehyde calibration curves were established by vaporization of liquid solutions with
192 concentrations from 250 to 8000 mg/L under steam atmosphere (between 2250 cm^{-1} and 2850 cm^{-1}).
193 Ammonia calibration curves were established using ammonia gas tanks with different concentrations
194 of 500, 1000, and 5000 ppm under nitrogen atmosphere (between 910 cm^{-1} and 1150 cm^{-1}). All
195 calibrations were performed using the dilution system to avoid any error in the dilution ratio.

196 2.5 Steam-cooking pilot (depollution by hydrolysis at lab-scale in batch mode)

197 The steam cooking pilot used to perform the experiments is a combination of different apparatuses
198 (steam generator, reactor, furnace, and condensation system). The steam generator could produce
199 and maintain pressure up to 8 bars inside the reactor. The reactor is an inox 2.5-liter volume vessel,
200 which is placed inside an oven. A schematic view of the steam cooking pilot is presented in Fig. 2.



212

213

Figure 2. Steam cooking apparatuses schematic view

214 Inlet samples were introduced through the head of the reactor via a feed line. A manual quarter-turn
215 valve allowed the opening and closing of the supply line. For the extraction of the treated materials,
216 an automated quarter-turn valve made it possible to open the reactor via a horizontal pipe through
217 which the treated materials, under pressure, escaped and were collected at the base of the cyclone
218 which ensures the solid/vapor separation.

219 The reactor was supplied with steam (produced by a steam generator fitted with a pressure
220 regulator), and the pressure was measured using a needle gauge. In order to analyze on-line the
221 hydrolysis products, a steam leakage flow is controlled through a needle valve. The steam flow allows
222 also to evaluate the effect of the steam ratio which is given as the ratio between steam flow and the
223 mass of waste sample used for the test ($g_{\text{steam}}/\text{min}/g_{\text{wood waste}}$). A condensation system composed of
224 two coolers in series supplied with cold water by a high-power cryostat (Unichiller 022-H-MPC with a
225 maximum power of 3335W) is positioned at the outlet of the polluted steam flow line. The
226 condensed liquid was then collected in a container weighed by a scale connected to a computer
227 which calculates and records continuously instant steam flow rate. The condensation system thus
228 designed allows a maximum condensation flow rate of $30 g_{\text{steam}}/\text{min}$.

229 A tiny part of the polluted vapors is automatically sampled to feed the gas measurement device
230 (dilution system + FTIR spectrometer). This sampling flow is assumed largely lower than the steam
231 leakage one, ensuring a good steam leakage flow measurement. The gases leaving the reactor
232 consists mainly of water vapor (not far from 99%) which makes it impossible for the on-line gas
233 analysis by FTIR measurement (.due to the broad band of water adsorption in the infra-Red). This is
234 why a dilution system was used to dilute the gas to be analyzed (dilution rate close to 100).
235 Preliminary tests have shown the effectiveness of the method.

236 Regarding the dosage of formaldehyde, quantifications were also carried out by HPLC on the liquid
237 phase collected to verify the accuracy of the measurement by IRTF. Concerning the one ammonia,
238 nitrogen balance was performed by measuring nitrogen content in solids before and after
239 experiments.

240 Two parameters were tested during the experiments: The temperature/pressure couple and the
241 steam ratio ($g_{\text{steam}}/\text{min}/g_{\text{waste}}$). Regarding the temperature-pressure couple, the temperature of the
242 oven was always set at a few degrees above the dew temperature (according to steam pressure) to
243 avoid any condensation of the steam in the reactor and, therefore to work under dry steam.

244 2.6 Tested conditions

245 Tests in different conditions were performed to evaluate the effects of pressure/temperature couple
246 as well as steam ratio. Close to all tests were performed with 40g of waste sample. Because of the
247 limitation of steam leakage flow at $30 g_{\text{steam}}/\text{min}$, tests for 1.5 and $3 g_{\text{steam}}/\text{min}/g_{\text{waste}}$ steam ratios
248 were carried out with lower sample mass. The duration of each run was 1 hour. Tests were
249 triplicated and the average results are presented here. All tested conditions are summarized in table
250 1.

251

Table 1. Different conditions tested during the experiments

Pressure (bar)	Temperature	Wood waste	steam flow	Steam ratio
----------------	-------------	------------	------------	-------------

		(°C)	dry mass (g)	(g _{steam} /min)	(g _{steam} /min/g _{waste})
Effect of temperature	2.5	139	40	30	0.75
	3.5	148	40	30	0.75
	4.5	155.5	40	30	0.75
	5.5	162	40	30	0.75
	6.5	168	40	30	0.75
Effect of steam ratio	3.5	148	40	10	0.25
	3.5	148	40	20	0.5
	3.5	148	40	30	0.75
	3.5	148	20	30	1.5
	3.5	148	10	30	3

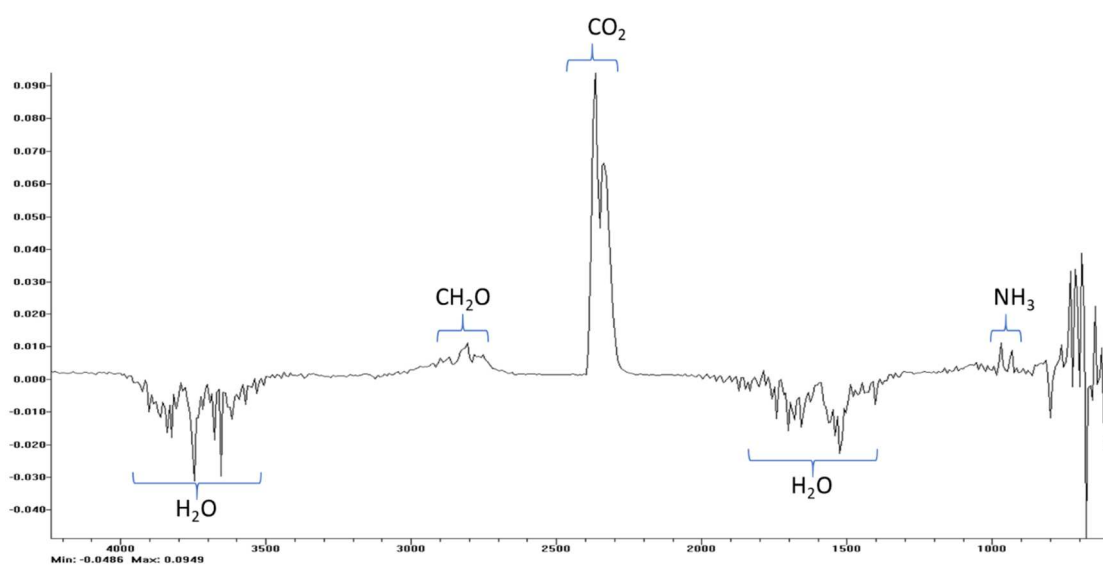
252

253 3. Results and discussion

254 3.1. Hydrolysis products characterization by on-line FTIR measurement

255 Fig. 3. shows the typical absorbance spectrum obtained by FTIR during the hydrolysis of wood waste
 256 during steam cooking. It appears that only three species are produced during degradation, at least in
 257 detectable quantities: carbon dioxide (double peak at 2650 cm⁻¹), ammonia (double peak at 950 cm⁻¹)
 258 ¹), and formaldehyde (around 2800 cm⁻¹). This is consistent with the literature (Wan et al., 2014;
 259 Hagel et al., 2020; Park et al., 2013; Ringena et al., 2006). Hagel et al. (2020) also reported the
 260 production of acids (acetic and formic), but their presence in the gas phase was not identified. It
 261 could be due to their too low concentration or to the fact that being less volatile than ammonia and
 262 formaldehyde, these compounds stay in a liquid state in these conditions.

263 Peaks corresponding to water vapor appear in negative (3500-4000 cm⁻¹ and 1400-1800 cm⁻¹). This
 264 point is expected because, in order to avoid the saturation of the water vapor response (present in a
 265 large majority in front of the other species), the blank (reference measurement) was carried out
 266 under pure water vapor (after dilution). The presence of the other constituents under test
 267 conditions, therefore, reduces the water content in comparison with the reference measurement,
 268 which explains the negative values.



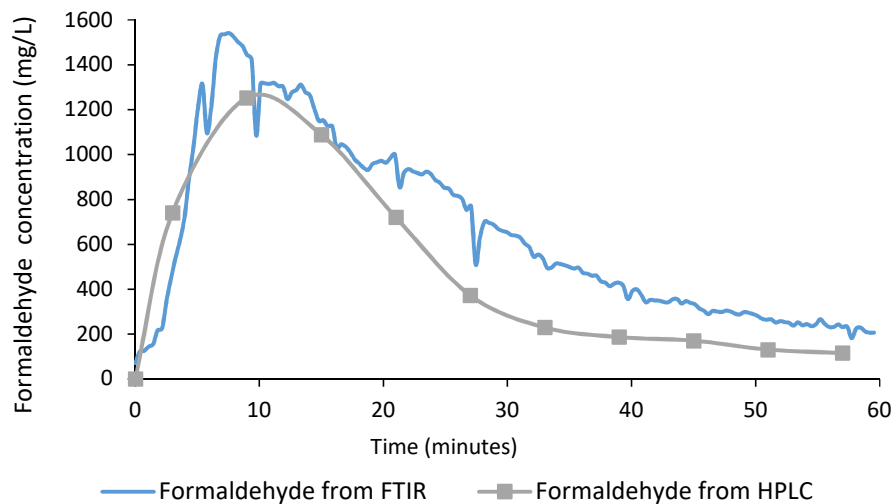
269

270

Figure 3. The infrared spectrum of wood waste degradation products by steam cooking

271 3.2. Confirmation of using FTIR as a replacement to HPLC for measurement of ammonia and
272 formaldehyde

273 Formaldehyde, which is transferred from the wood waste to the gas (as is liquidated in the
274 condenser), is generally measured by HPLC (Ihnát et al., 2017; Lee et al., 2014). However, since HPLC
275 measurement requires a long time for each sample, using FTIR directly for analyzing outlet steam
276 was tested. The test was performed at 3.5 bar, 10g/min steam flow, and 40g initial dried crushed
277 wood waste. Every 6 minutes, liquid samples are recovered for the HPLC test, while FTIR measures
278 formaldehyde and ammonia on-line. The result is shown in Fig. 4.



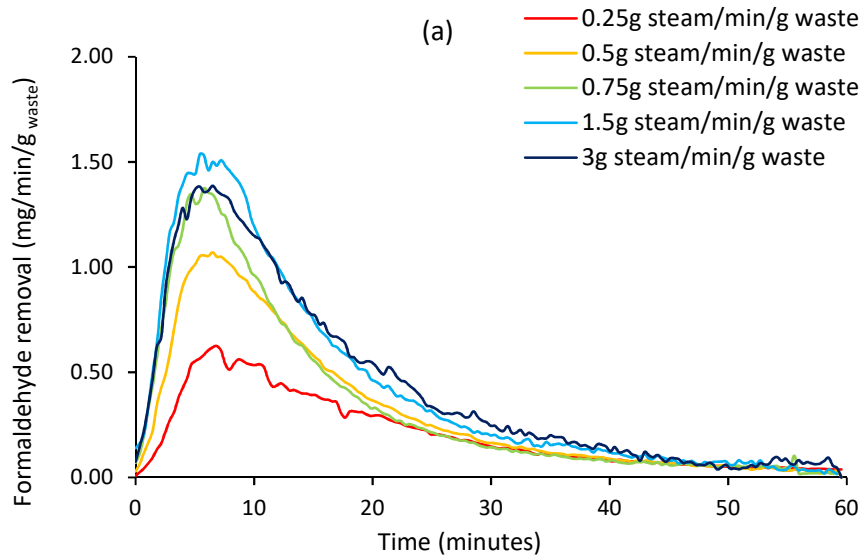
279

280 Figure 4. Comparing the concentration of formaldehyde during the steam cooking test measured by HPLC and FTIR

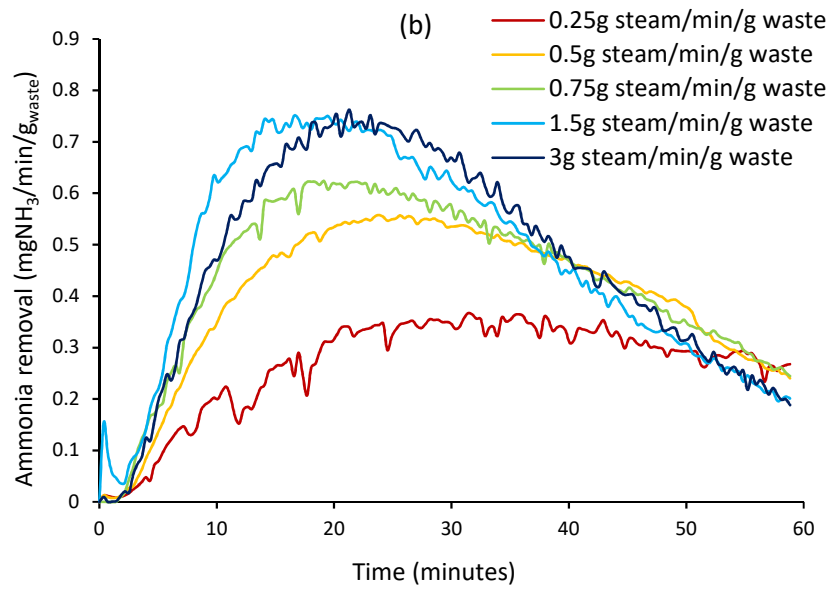
281 As shown in Figure 4, the results obtained from HPLC and FTIR are reasonably close to each other.
282 Therefore, for the rest of the tests, FTIR is used to measure the outlet steam directly.

283 3.3 Effect of Steam ratio on steam cooking of wood waste

284 The first studied parameter was the steam ratio. Fig. 5 (a) and (b) show the results of formaldehyde
285 and ammonia removal. As it can be seen from the curves below, whether for formaldehyde or
286 ammonia, the flow of pollutants eliminated during the tests increases rapidly before decreasing
287 throughout the test. The elimination of formaldehyde is almost complete at the end of the test in
288 one hour, while this is not the case for ammonia.



289



290

291

Figure 5. (a) Formaldehyde and (b) ammonia emissions as a function of time and steam/wood waste ratio.

292

Integrating these curves makes it possible to determine the total amount of formaldehyde and

293

ammonia removed during the test. The results can be seen in Fig. 6.

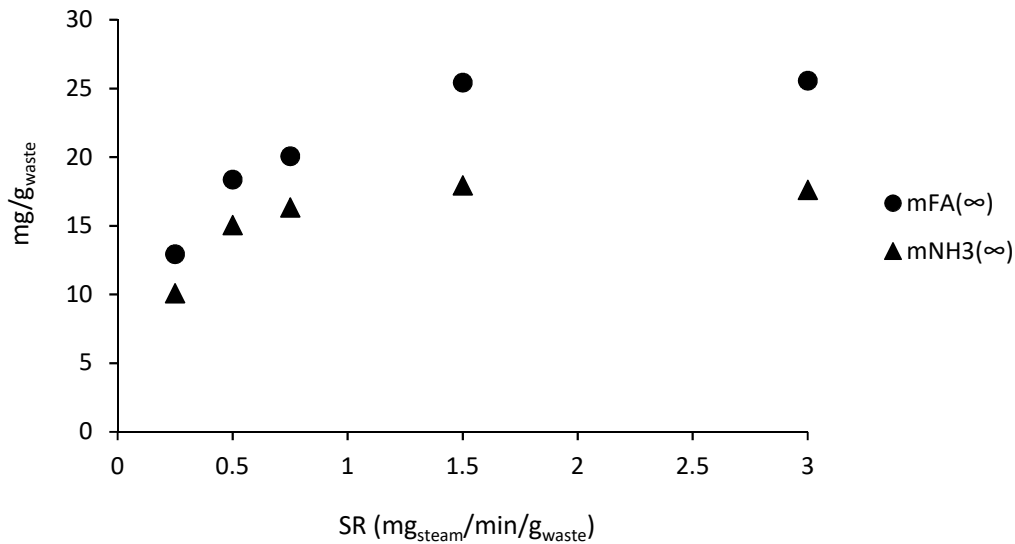


Figure 6. Effect of steam ratio (SR) on the total removal of formaldehyde and ammonia.

294

295

296 It can be seen that by increasing the flow per gram of initial mass, the total mass of both ammonia
 297 and formaldehyde increases until a certain point (over 1.5 steam ratio values). The quantity of
 298 formaldehyde released is in the range of 13 to 25.5 mg per gram of waste while the one of ammonia
 299 is between 10.1 to 17.6 mg_{NH₃}/g_{waste}. Comparing these results with the literature is difficult since, to
 300 our knowledge, no article reports results concerning ammonia and formaldehyde released in the gas
 301 phase. All references dealing with the hydrolysis of UF resin (Myers and Koutsky, 1990; Ringena et al.,
 302 2006; Park and Jeong, 2011; Park and Causin, 2013; Lubis and Park, 2018; Grigsby et al., 2014), wood
 303 waste such as Particleboard (Lykidis and Grigoriou, 2008; Wan et al., 2014), and MDF (Wan et al.,
 304 2014; Hagel and Saake, 2020; Lubis et al., 2018; Lubis et al., 2020; Kraft and Roffael, 2003; Grigsby et
 305 al., 2014) present analyzes of the hydrolysate in the liquid phase. Some studies carried out in the
 306 liquid phase were at atmospheric pressure and not under pressurized steam (Lykidis and Grigoriou,
 307 2008; Wan et al., 2014; Hagel and Saake, 2020).

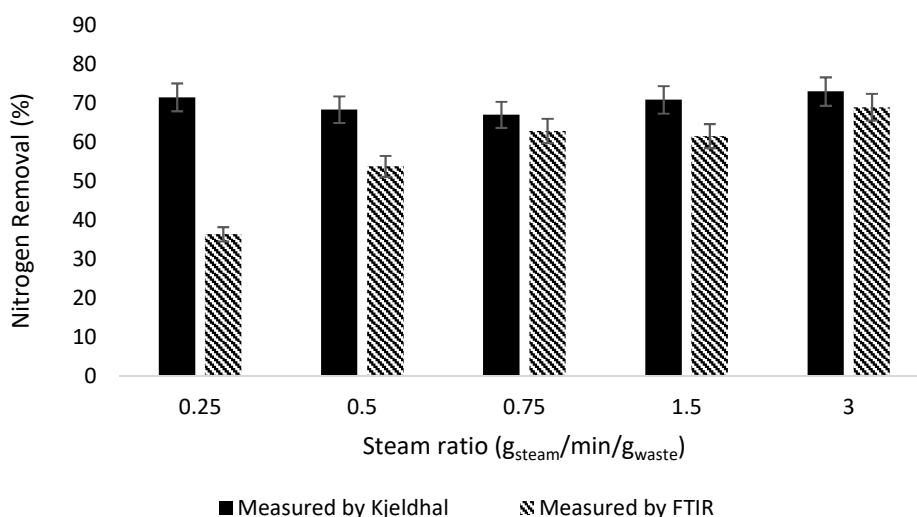
308 Nevertheless, not all data from different studies can be compared. Concerning ammonia, it is
 309 reported that the formation of free ammonia from the degradation of cured UF resins leads to the
 310 formation of ammonium ions (NH₄OH⁻) in the solution and an increase in the pH of the extract
 311 solution (Lubis and Park, 2018; Lubis et al., 2021). Only the pH of the solution is therefore measured
 312 as an indicator of ammonia production, but it remains a qualitative analysis. Moreover, a
 313 competition between acid release by wood hydrolysis (acetic and formic acid) in severe conditions
 314 and ammonia production makes it impossible to use only pH to quantify ammonia production (Hagel
 315 and Saake, 2020).

316 Another possible way to quantify ammonia is nitrogen titration in the liquid phase. Some authors
 317 (Lubis and park, 2018; Lubis et al., 2020; Kraft and Roffael, 2003; Grigsby et al., 2014) report such
 318 measurements, but the calculation of ammonia production is never have been done. Only nitrogen
 319 balance is performed to evaluate the reliability of the results.

320 Concerning formaldehyde release, different studies (Ringena et al., 2006; Park and Lee, 2015; Lubis
 321 and Park, 2018; Lubis et al., 2020) report formaldehyde titration in the liquid phase, but tests were
 322 performed on UF resin and not on waste wood. Values reported vary between 1 to 70 mg/g of resin;
 323 still, it remains difficult to compare. Lykidis and Grigoriou, 2008 and Wan et al., 2014, who worked on
 324 wood waste steam hydrolysis, only measured the free formaldehyde emissions at the surface of
 325 panel boards produced with the hydrolysed waste wood. Only Kraft and Roffael, (2003), who studied

326 the hydrolysis of MDF samples in water at a temperature between 100°C and 130°C (pressure not
327 defined) for 20 minutes, reported formaldehyde release between 21.6 to 34.2 mg/g of waste which is
328 quite similar to results provided in the presented study.

329 To evaluate the accuracy of FTIR measurement, a comparison between the nitrogen removal rate
330 (wt. %) calculated from online gas analysis and from solid analysis (nitrogen content before and after
331 steam cooking measured by Kjeldahl analysis) is performed. which the result is shown in Fig. 6. Even
332 if values are quite similar (except for the 0.25 steam ratio), it is noticeable that the trends given by
333 FTIR analysis (an increase of the nitrogen removal with steam ratio) are no more discernable with
334 results obtained through Kjeldahl analysis. This point could be explained by the fact the loss of mass
335 during the test has not been taken into account in the calculation of the nitrogen removal through
336 Kjeldahl analysis. Fig. 7 shows that the sum of the mass of formaldehyde and ammonia removed
337 during the test per gram of sample is between 23 to 43 mg which corresponds to 2.3 to 4.3% of mass
338 loss. The characterization of hydrolysis production in part 3.1 also reveals the presence, in low
339 quantities, of carbon dioxide which conducts to a higher loss of mass. Taking into account this
340 increasing mass loss with steam ratio, it can be assumed that the nitrogen removed calculated from
341 the solid analysis will therefore follow the same trends like the one obtained with FTIR
342 measurements.



343

344 Figure 7. Comparison of nitrogen removal using the Kjeldahl method and FTIR analysis according to steam ratio.

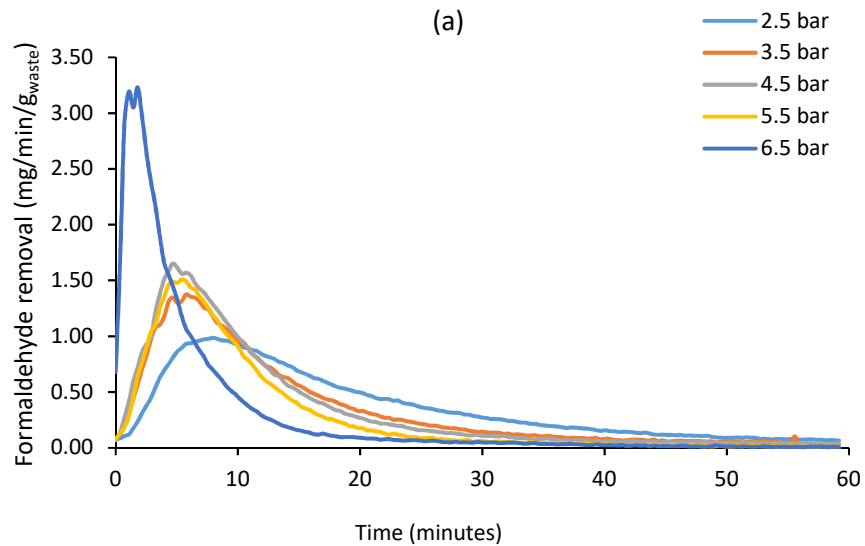
345

346 The percentage of nitrogen eliminated is between 36.4 and 69%, according to the results obtained by
347 gas analysis, while it is about 70% according to the analysis of solids. Considering the loss of mass of
348 the samples, the values obtained by analysis of the solids would tend to increase. This indicates that
349 the nitrogen removal rate is either overestimated by the solid analysis or underestimated by the gas
350 analysis. It is quite difficult to conclude the origin of these discrepancies. Nevertheless, these values
351 are consistent and in agreement with Lubis et al. (2018) who reported a nitrogen removal in the
352 range of 40 to 80% for 2 hours for a MDF sample hydrolysis test in water between 40°C and 100°C.

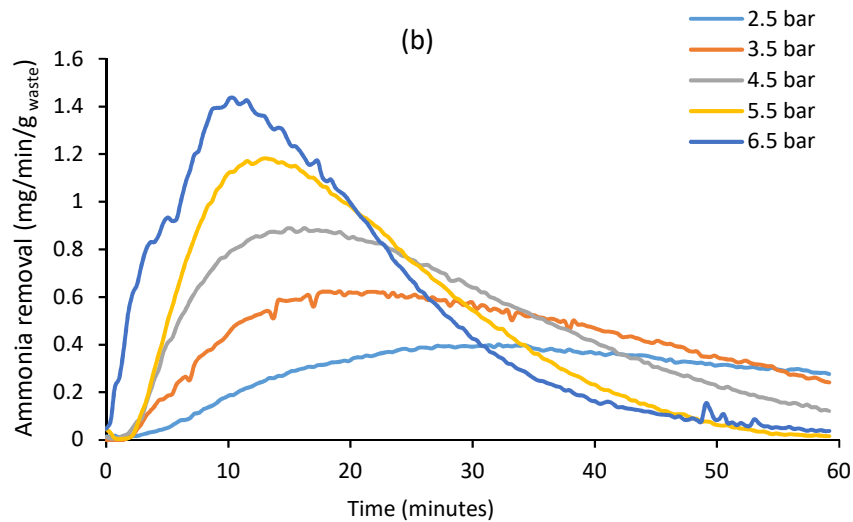
353

354 3.4 Effect of pressure/temperature on steam cooking of wood waste

355 The next studied parameter was the pressure/temperature couple. The results can be seen in Fig. 8
356 (a) and (b). It is clear from these curves that pressure/temperature has a positive effect on the rate of
357 pollutant removal in the same way.



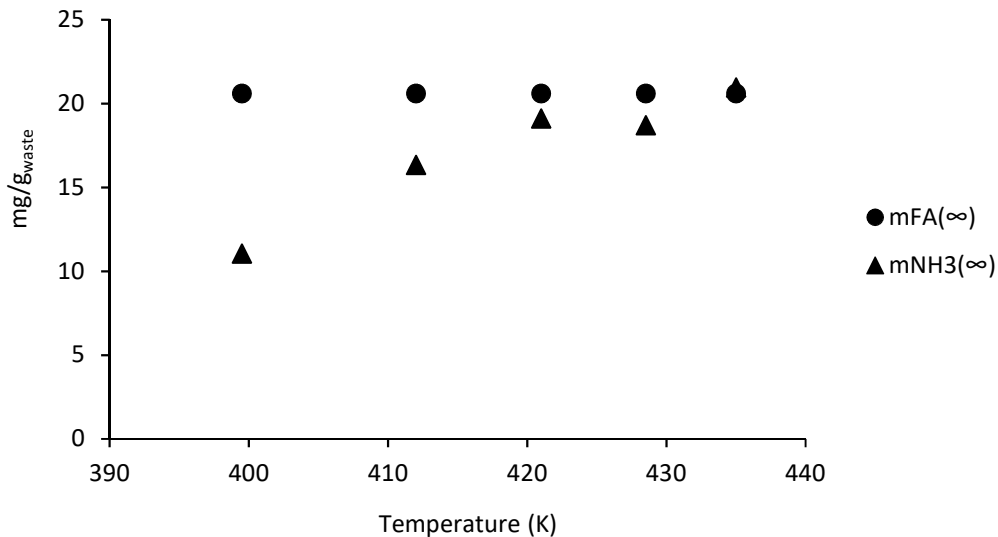
358



359

360 Figure 8. Effect of pressure/temperature on (a) formaldehyde and (b) ammonia removal from wood waste.

361 As previously explained, the total quantity of formaldehyde and ammonia eliminated during each
362 test is determined by integrating the curves. The results are shown in Fig. 9.



363

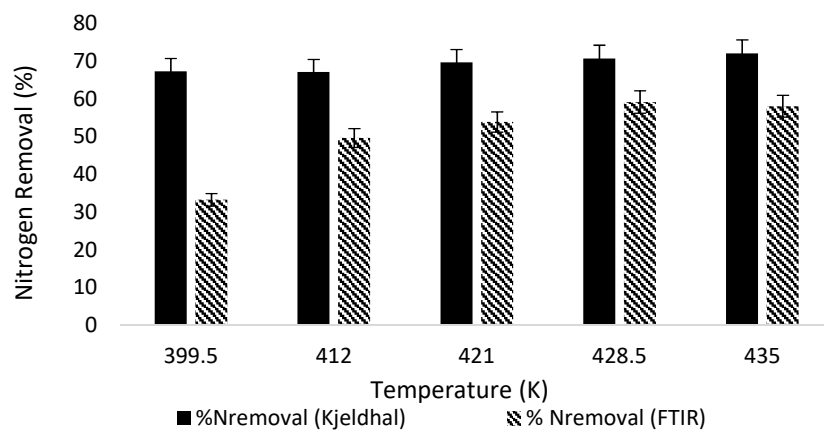
364

Figure 9. Effect of temperature on the total removal of formaldehyde and ammonia.

365 From the results obtained above, it can be interpreted that whatever the conditions were,
 366 formaldehyde elimination was almost complete after one hour of the experiment. The total mass of
 367 formaldehyde is independent of the temperature and reaches 20.6 mg of formaldehyde per gram of
 368 waste.

369 Regarding ammonia, elimination is almost complete for the two highest pressures (5.5 and 6.5 bars),
 370 while it is not complete for the lower pressures. The mass of ammonia eliminated increases with
 371 pressure. However, it is difficult at this stage to say whether this is an effect of the
 372 pressure/temperature or whether it is only because the reaction does not have enough time to
 373 complete over the entire duration of the test. The released quantities of ammonia are between 11 to
 374 21 mg_{NH₃} /g_{waste}.

375 Fig. 10 shows the evaluation of the reliability of FTIR measurements. The conclusions are entirely
 376 similar to the conclusions made in the previous paragraph. The trend of increasing nitrogen removal
 377 rate with the severity of treatment with gas analysis (from 33.2 to 58.1%) is much less in comparison
 378 to the results obtained by solids analysis (67 to 72%). This is due to the fact that mass loss was not
 379 taken into account during the tests. Similarly, a significant difference is observed between the values
 380 obtained by solids analysis, which are overestimated compared to gas analysis. The results are
 381 consistent and comparable to those obtained by Lubis et al. (2018).



382

383

Figure 10. Comparison of nitrogen removal using the Kjeldahl method and FTIR analysis according to temperature.

384 3.4 Modelling ammonia and formaldehyde removal from wood waste

385 3.4.1 Description of the model

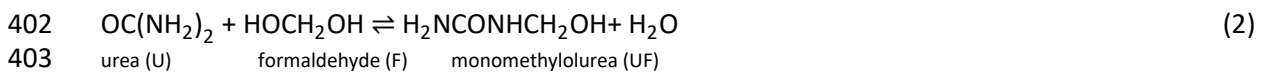
386 It is tried here to find a model which describes as best as possible emissions of both formaldehyde
387 and ammonia from wood waste through hydrolysis according to experiments operatory conditions.
388 The modeling will not concern the tests for a steam ratio of 1.5 and 3 as the masses of the samples
389 are not 40g.

390 Initially, it was considered that the wood waste consists of wood and UF resin. Therefore:
391 wood waste = $\lambda_W \times \text{wood} + \lambda_R \times \text{Resin}$ (1)

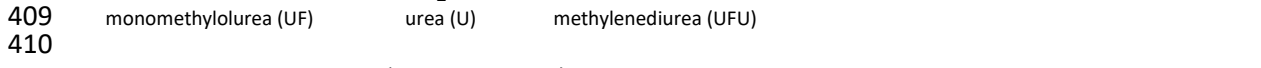
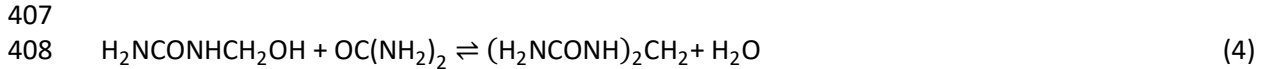
392 λ_W and λ_R are the relative mass contents of wood and resin respectively in $\frac{g_{\text{wood}}}{g_{\text{wood waste}}}$ and
393 $\frac{g_{\text{resin}}}{g_{\text{wood waste}}}$.

394 The model consists of numerically evaluating the production rates ($g_{\text{compound}}/\text{min}/g_{\text{waste}}$) and the
395 cumulative masses ($g_{\text{compound}}/g_{\text{waste}}$) of formaldehyde and ammonia emitted during the hydrolysis
396 reaction. These species are emitted during the degradation of the UF resin and not of the wood, so
397 the model is focused only on the degradation of the resin and not that of the sample as a whole.

398 According to the literature (Myers, 1986), the crosslinking of UF resins takes place according to
399 several (reversible) dehydration reactions, which take place simultaneously in series and in parallel to
400 form increasingly high molecular weight urea and formaldehyde polymers. Examples of these
401 reversible reactions, for lower molecular weights, are given here:

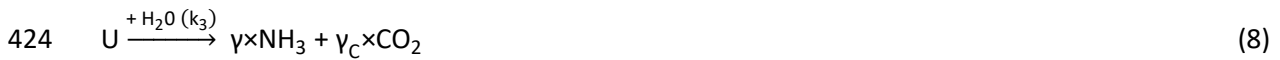


404



413 A very simplified reaction mechanism is then proposed to describe the hydrolysis phenomenon of
414 the resin present in the waste. The solid R (resin) is modified during a first hydrolysis reaction to give
415 an intermediate compound I without producing formaldehyde or ammonia. The intermediate
416 compound I then corresponds to the partially depolymerized resin. In turn, it degrades during
417 reaction 2 into urea (U) and formaldehyde (FA). Urea is then finally degraded into gaseous ammonia
418 (NH_3) and carbon dioxide (CO_2) during reaction 3. α , β_{NH_3} , β_{FA} , γ and γ_C correspond respectively to
419 the masses of I (partially depolymerized resin), U, FA, NH_3 , and CO_2 produced per unit mass of parent
420 compounds. Thus, the units of α , β_{NH_3} , β_{FA} , γ and γ_C are respectively g_I/g_R , g_U/g_I , g_{FA}/g_I , g_{NH_3}/g_U ,
421 and g_{CO_2}/g_U . The reaction mechanism can thus be outlined as below:





425 Assuming that the kinetic laws of degradation are in first order with respect to the reactants and in
 426 zero-order with respect to the water vapor (present in large quantities and therefore content is
 427 stable during the reaction), the material balances of the compounds are as follows:

428 • Solids (resonated on the mass–closed system): $\left(\frac{g_{\text{compound}}/\text{min}}{g_{\text{waste}}} \right)$

429 $\frac{dm_R(t)}{dt} = -k_1 \times m_R(t)$ (9)

430 $\frac{dm_I(t)}{dt} = \alpha \times k_1 \times m_R(t) - k_2 \times m_I(t)$ (10)

431 $\frac{dm_U(t)}{dt} = \beta_{NH_3} \times k_2 \times m_I(t) - k_3 \times m_U(t)$ (11)

432 • Gas (resonated on the density – open system): $\left(\frac{g_{\text{compound}}/\text{min}}{g_{\text{waste}}} \right)$

433 $Q \times \rho_i$ represents the flow rate of species leaving the reactor through the outlet pipe;

434 $V_g \times \frac{d\rho_i(t)}{dt}$ represents the variation of the mass of species within the reactor;

435 With V_g , the reactor volume (2.5 L) and Q , the steam flow in L/min (taking into account the
 436 temperature and pressure conditions within the reactor). The analytical integration of the differential
 437 equations is not essential, a so-called “iterative” numerical method is used here. Knowing the initial
 438 value of each of the masses (or densities) ($R(0) = \lambda_R$; $I(0) = U(0) = \rho_{NH_3}(0) = \rho_{FA}(0) = 0$), the initial value
 439 of the variation rate of the mass (or density) of species can be determined ($\frac{dm_i(0)}{dt}$ or $\frac{d\rho_i(0)}{dt}$).
 440 Considering this value remains constant between two measurement steps (iteration step = 0.1
 441 minutes), the value of the quantities at the next iteration step can then be determined by the
 442 following equation:

443 $m_{i(n+1)} = m_{i(n)} + \frac{dm_{i(n)}}{dt} \times \Delta t$, with Δt the sampling time; $\Delta t = 0.1$ min

444 The production rates of formaldehyde and ammonia $\left(\frac{g_{\text{compound}}/\text{min}}{g_{\text{waste}}} \right)$ emitted during the
 445 hydrolysis reaction as a function of time are represented by the term $Q \times \rho_i(t)$. The cumulative masses
 446 $\left(\frac{g_{\text{compound}}}{g_{\text{waste}}} \right)$ of formaldehyde and ammonia emitted per unit mass of sample during the
 447 hydrolysis reaction are determined according to the following equation:

448 $m_i(t+\Delta t) = m_i(t) + Q \times \rho_i(t)$ (15)

449 For each experimental condition, error functions (sum of the squared difference between the
 450 calculated and the experimental values) on the production rates ($erfc dm_{NH_3}$ and $erfc dm_{FA}$) are
 451 calculated. These different error functions can be added as needed to optimize the desired

452 parameters according to the different tests to be taken into account. All errors obtained are
 453 summarized in Table 2.

454

455

Table 2. Error function table

		NH₃		FA
T°C	T(K)	SR	erfc dm_{NH3}	erfc dm_{FA}
148	412	0.25	1.85	1.58
148	412	0.5	0.93	1.30
148	412	0.75	0.10	2.39
Sum "Effect SR"			2.88	5.27
139	412	0.75	0.35	5.43
148	421	0.75	0.10	2.39
155.5	428.5	0.75	0.31	6.63
162	435	0.75	2.85	34.30
168	441	0.75	2.71	49.52
Sum "Effect T"			6.32	98.27
Sum "Effect SR and T"			9.20	103.54
Global sum of error functions			112.74	

456

457

458

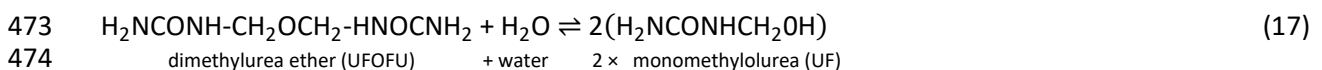
459 3.4.2 Determination of the parameters of the model

460 3.4.2.1 Determination of parameters α and γ (constants)

461 α , represents the ratio between the mass of the intermediate compound I produced (M_I) and the
 462 mass of the compound R consumed (M_R):

463
$$\alpha = \frac{M_I}{M_R} \quad (16)$$

464 The first reaction of the proposed reaction mechanism (eq 6) is considered representative of the
 465 depolymerization of the resin (by hydrolysis) without the production of urea, formaldehyde, or
 466 ammonia. This reaction can then be similar to the breaking of methylene ether bridges by hydrolysis
 467 (inverse of the fourth reaction for the production of dimethylurea ether (eq 5)). These are present
 468 throughout the cross-linked network of the UF resin and do bind not only resin monomers
 469 (monomethylolurea) but also dimers, trimers as well as a wide variety of fragments of varying
 470 degrees of polymerization. The precise determination of the parameter α is therefore theoretically
 471 impossible. Nevertheless, by doing the calculation for the case of the fourth reaction (Eq. 5) written
 472 in the direction of hydrolysis this time, the following equation can be obtained:



475 The first reaction of the proposed mechanism (eq 6) reacting one mole of compound R with one
 476 mole of water to give one mole of compound I, which can be explained as below:

477
$$M_I = M_R + M_{\text{H}_2\text{O}} \quad (18)$$

478 Thus, by combining equations (16) and (18):

479
$$\alpha = \frac{(M_R + M_{H_2O})}{M_R} \quad (19)$$

480 Considering that R represents the UFOFU dimer and based on equation (19), the following equation
481 can be obtained:

482
$$\alpha = \frac{(M_{UFOFU} + M_{H_2O})}{M_{UFOFU}} = \frac{(162 + 18)}{162} = 1.11 \quad (20)$$

483 In this specific case, the value of α is 1.11. For the other cases, which necessarily involve fragments of
484 larger molecular weights, the value of α will decrease and tend towards 1 for the highest molar
485 masses. Thus, even if the value of α cannot be calculated precisely, it is between 1 and 1.11.
486 Therefore, it was set to 1 for convenience. The reaction is then considered as depolymerization
487 without gaining mass, at least not significant given the high molecular weight of the resin fragments.
488 The value of α is not decisive for the model.

489 Regarding γ , it is worth considering the last reaction of the proposed mechanism (eq 8), which
490 describes the hydrolysis of urea into ammonia and carbon dioxide:



493 For 1g of urea consumed, 0.567g of ammonia (34/60) is produced. Therefore, the value of γ is set to
494 0.567.

495 3.4.2.2 Determination of other model parameters:

496 Determination of the parameters value and the kinetic constants was carried out according to
497 different methods based on different hypotheses:

- 498 • Case 1: The rate constants k_i only depends on the temperature;
499 ○ Case 1-a: β_{NH_3} and β_{FA} are variable; λ_R , α , and γ are constants
500 ○ Case 2-a: λ_R is variable; β_{NH_3} and β_{FA} are constants
501 • Case 2: The rate constants k_i depends on the temperature and steam ratio. Other parameters
502 remain constant.

503 3.4.2.2.1 Case 1-a:

504 The rate constants k_1 , k_2 , and k_3 only depend on the temperature according to the Arrhenius law:

505
$$k_i(T) = k_{0i} \times \exp\left(\frac{-E_{a_i}}{R.T}\right) \quad (22)$$

506 In order to account for the effect of the vapor ratio (SR) on the final quantities of formaldehyde and
507 ammonia emitted, the values of specific parameters are dependent on SR.

- 508 • λ_R : λ_R is the theoretical mass content of resin. Based on particleboard and MDF content in
509 waste wood, the UF glue content as the resin is around 10%. Knowing that in the batch of
510 wood waste used in this study, the rate of particleboard and fiberboard is around 80%, the
511 UF resin content in the samples is then around 8%. The value of λ_R is then fixed at 0.08
512 $\frac{g_{resin}}{g_{wood\ waste}}$ knowing that this value is not decisive.
513 • β_{NH_3} and β_{FA} : these parameters are independent of temperature but dependent on the value
514 of the steam ratio. Therefore, it was decided to use the cumulative masses of formaldehyde
515 and ammonia experimentally measured during the experimental tests. According to the

516 numerical model proposed, for 1 g of wood waste, the theoretical masses ($\frac{g_{\text{compound}}}{g_{\text{waste}}}$)
 517 at infinity mass of formaldehyde $m_{\text{FA}}(\infty)$ and of ammonia $m_{\text{NH}_3}(\infty)$ are equal to:

$$518 \quad m_{\text{FA}}(\infty) = \lambda_{\text{R}} \times \alpha \times \beta_{\text{FA}} \quad (23)$$

$$519 \quad m_{\text{NH}_3}(\infty) = \lambda_{\text{R}} \times \alpha \times \gamma \times \beta_{\text{NH}_3} \quad (24)$$

520 It appears here that the values of λ_{R} and α are not decisive as the parameters β_{NH_3} and β_{FA} will be
 521 determined from the experimental values of the theoretical masses when hydrolysis is completed
 522 and from the product $\lambda_{\text{R}} \times \alpha$. Thus, if the value of this product is changed, the values of β_{NH_3} and β_{FA}
 523 will be changed proportionally without changing anything in the model. Since this cannot be
 524 determined experimentally, it is impossible to verify whether the value of the various parameters is
 525 correct. It is only the value of the product of these different parameters that influence the result in
 526 terms of the amount of ammonia and formaldehyde produced. For formaldehyde, the values of
 527 $m_{\text{FA}}(\infty)$ according to the different parameters are known as the reaction is complete after of
 528 experiment period regardless of the conditions. The values of β_{FA} can then be deduced from the
 529 experimental values according to the expression:

$$530 \quad \beta_{\text{FA_exp}}(T, \text{SR}) = \frac{m_{\text{FA}}(\infty)(T, \text{SR})}{(\lambda_{\text{R}} \times \alpha)} \quad (25)$$

531 An evolution in logarithmic form makes it possible to adequately describe the evolution of β_{FA} as a
 532 function of steam ratio using the following equation:

$$533 \quad \beta_{\text{FA_Calc}} = 0.1082 \times \ln(\text{SR}) + 0.2886 \quad (26)$$

534 The values of $\beta_{\text{FA_Exp}}$ and $\beta_{\text{FA_Calc}}$ are presented in Table 3.

535 Table 3. Values of $\beta_{\text{FA_Exp}}$, $\beta_{\text{FA_Calc}}$, $\beta_{\text{NH}_3_Opt}$ and $\beta_{\text{NH}_3_Calc}$

SR	T (°C)	T (K)	$m_{\text{FA}}(\infty)$	$\beta_{\text{FA_exp}}$	$\beta_{\text{FA_calc}}$	$m_{\text{NH}_3}(\infty)$	$\beta_{\text{NH}_3_opt}$	$\beta_{\text{NH}_3_calc}$
0,25	148	421	0,01295	0,1619	0,1387	0,0101	0,2225	0,2830
0,5	148	421	0,01837	0,2296	0,2136	0,0151	0,3322	0,3961
0,75	148	421	0,0206	0,2575	0,2575	0,0164	0,4621	0,4623
0,75	139	412	0,0206	0,2575	0,2575	0,0111	0,4621	0,4623
0,75	148	421	0,0206	0,2575	0,2575	0,0164	0,4621	0,4623
0,75	155.5	428.5	0,0206	0,2575	0,2575	0,0191	0,4621	0,4623
0,75	162	435	0,0206	0,2575	0,2575	0,0187	0,4621	0,4623
0,75	168	441	0,0206	0,2575	0,2575	0,0210	0,4621	0,4623

536 For ammonia, the values of $m_{\text{NH}_3}(\infty)$ as a function of the various parameters are unknown as the
 537 reaction is not complete at the end of the experiment period except for the test at 435K for a steam
 538 ratio of 0.75. For this condition, the value of $\beta_{\text{NH}_3_Exp}(0,75)$ can then be deduced from the
 539 experimental value according to the following expression:

$$540 \quad \beta_{\text{NH}_3_Exp}(0,75) = \frac{m_{\text{NH}_3}(\infty)(435 ; 0,75)}{(\lambda_{\text{R}} \times \alpha \times \gamma)} = \frac{0,0209}{(0,08 \times 1 \times 0,567)} = 0,462 \quad (27)$$

541 The values of β_{NH_3} for the other values of steam ratio will then be obtained by optimization. Knowing
 542 the values of the different parameters of λ_{R} , α , and β_{FA} , the optimization of the kinetic parameters
 543 k_{01} , E_{a1} , k_{02} , and E_{a2} is carried out by minimizing the sum of the error functions obtained for
 544 formaldehyde on the production rate ($\text{erfc } dm_{\text{FA}}$) for conditions where the temperature is variable

545 (yellow box on table 2). Knowing only the value $\beta_{\text{NH}_3_Exp}$ (0.75) = 0.462 for a steam ratio of 0.75, the
 546 values of the kinetic parameters k_{03} and E_{a3} are optimized only for the tests with a steam ratio of 0.75
 547 and with temperatures variables by minimizing the sum of the error functions obtained for ammonia
 548 on the production rate ($erfc_{dm_NH_3}$, the orange box on table 2). The values of the β_{NH_3} for the different
 549 values of steam ratio are optimized one by one. Knowing the evolution of the values of $\beta_{\text{NH}_3_Opt}$ as a
 550 function of steam ratio, an equation is used to calculate these values as a function of steam ratio
 551 according to the following expression:

$$552 \quad \beta_{\text{NH}_3_Calc} = A \times \ln(\text{SR}) + B \quad (28)$$

553 The constants A and B as well as the kinetic parameters k_{03} and E_{a3} are finally optimized
 554 simultaneously for all the tests (green box on table 2).

$$555 \quad \beta_{\text{NH}_3_Calc} = 0.1632 \times \ln(\text{SR}) + 0.5093 \quad (29)$$

556 The values of $\beta_{\text{NH}_3_Opt}$ and $\beta_{\text{NH}_3_Calc}$ are listed in Table 3.

557 The velocity laws are assumed to be of zero-order concerning the water vapor, assumed to be in
 558 large quantities. As a result, the values of k determined previously are "apparent" values and the
 559 "real" k depends on the density of the water vapor pressure under the conditions of the various
 560 tests:

$$561 \quad k_{\text{apparent}} = k_{\text{real}} \times \rho_{\text{water}} \quad (30)$$

562 Based on the ideal gas law, the density of water according to the experimental conditions (Pressure
 563 and Temperature) is calculated with the following equation:

$$564 \quad \rho_{\text{water}}(P, T) = \frac{P \times M_{\text{water}}}{RT} \quad (31)$$

565 The value of $k_{i_apparent}$ is then divided by the density of the saturation vapor pressure ρ_{water} for the
 566 conditions of the various tests. The k_{i_real} of the three reactions is plotted as $\ln(k_{i_real}) = f(1/T)$ to
 567 determine the new values of k_{0i_real} and E_{ai_real} .

568

569 3.4.2.2.2 Case 1-b:

570 As it was shown that the evolution trends of β_{NH_3} and β_{FA} values follow a similar shape, it is expected
 571 that evolution trends for λ_R could also be represented by a logarithmic form according to the eq (32):

$$572 \quad \lambda_R = C \times \ln(\text{SR}) + D \quad (32)$$

573 λ_R is then no longer considered as the resin content in the waste but as the reactive part of the resin,
 574 which depends only on the value of the steam ratio. The kinetic constants k_{0i_real} and E_{ai_real} remain
 575 unchanged as do the values of α and γ . The values used for β_{NH_3} and β_{FA} , those obtained for an steam
 576 ratio of 0.75 are $\beta_{\text{NH}_3}=0,462$ $\beta_{\text{FA}}=0,2575$. The values of C and D are optimized by minimizing the
 577 global sum of the error functions on the production rate (grey boxes in table 2):

$$578 \quad \lambda_R = 0.0313 \times \ln(\text{SR}) + 0.0887 \quad (33)$$

579 3.4.2.2.3 Case 2:

580 The values of λ_R , α , and γ remain unchanged from case 1-a ($\lambda_R=0.08$; $\alpha=1$; $\gamma=0.567$). The values used
 581 for β_{NH_3} and β_{FA} are those obtained for a steam ratio of 0.75 ($\beta_{\text{NH}_3}= 0.462$, $\beta_{\text{FA}} = 0.2575$). The rate

582 constant k_{1_real} follows Arrhenius law; It is therefore only dependent on the temperature and not on
 583 the steam ratio:

$$584 \quad k_{1_real}(T) = k_{01_real} \times \exp\left(\frac{-E_{a1_real}}{R.T}\right) \quad (34)$$

585 The rate constants k_2 and k_3 are both dependent on T (according to Arrhenius law) and steam ratio:

$$586 \quad k_{i_real}(T) = k_{0i_real} \times \exp\left(\frac{-E_{a_i_real}}{R.T}\right) \times \exp\left(\frac{-H_i}{SR}\right) \quad (35)$$

587 The dependence of the constants k_2 and k_3 with respect to the value of the steam ratio is explained
 588 by taking into account transfer phenomena at the surface of the sample. By increasing the ratio of
 589 water vapor to the mass of the sample (SR), the concentration of water vapor at the surface of the
 590 sample increases which leads to an increase in the rate of the reaction.

591 The values of the parameters λ_R , α , and β_{FA} being known, the kinetic parameters k_{01} , E_{a1} , k_{02} and E_{a2}
 592 (dependence of k_1 and k_2 as a function of T) and the parameter relating to the dependence of k_2 with
 593 the value of steam ratio (H2) are optimized by minimizing the sum of the errors obtained for
 594 formaldehyde on the production rate (box in yellow in Table 2). The value of β_{FA} is then optimized
 595 and obtained as $\beta_{FA} = 0.237$.

596 The values of the parameters λ_R , α , γ , and β_{NH3} are known. The kinetic parameters k_{03} and E_{a3}
 597 (dependence of k_3 as a function of T) and the parameter relating to the dependence of k_3 with the
 598 value of the steam ratio (H3) are optimized by minimizing the sum of the errors obtained for
 599 ammonia both on the cumulative mass and on the production rate (box in orange in the table of
 600 errors). The value of β_{NH3} is then optimized and obtained as $\beta_{NH3} = 0.476$.

601 3.4.3 Presentation and comparison of model results:

602 All the model parameters for the different cases studied are listed in Tables 4 and 5. The three
 603 approaches considered for the model made it possible to represent the production of formaldehyde
 604 and ammonia as a function of time and the cumulative masses eliminated during the tests for all
 605 assessed conditions. Here only the curves relating to Case 1-b are shown to avoid confusion (Fig. 11
 606 to 14).

607 Table 4. Kinetic parameters of the model for the 3 cases studied

		Case 1-a		Case 1-b		Case 2	
		K_{01}	E_{a1} or H_1	K_{01}	E_{a1} or H_1	K_{01}	E_{a1} or H_1
Temperature effect	Stage 1	3.36E+06	5.74E+04	3.36E+06	5.74E+04	1.25E+06	5.40E+04
	Stage 2	1.74E-01	4.35E+03	1.74E-01	4.35E+03	2.13E-01	2.44E+03
	Stage 3	2.77E+00	1.69E+04	2.77E+00	1.69E+04	6.29E+00	1.98E+04
Steam ratio effect	Stage 2						4.31E-01
	Stage 3		-		-		9.44E-02

608

609 Table 5. Stoichiometric parameters of the model for the three cases studied

	Case 1-a	Case 1-b	Case 2
λ_R	0,08	$0,0313 \times \ln(SR) + 0,0887$	0,08
α	1	1	1
γ	0,567	0,567	0,567

β_{FA}	$0,0882 \times \text{LN}(\text{SR}) + 0,2829$	0,258	0,237
β_{NH_3}	$0,1632 \times \text{LN}(\text{SR}) + 0,5093$	0,462	0,476

610

611 The comparison of the different modeling approaches can be made by comparing the values of the
612 sums of the error functions given in Table 6. The values of the overall errors on the production rates
613 for the three cases are very similar (between 112 and 113). On the other hand, the difference is more
614 marked when comparing the overall errors on the cumulative masses this time (between 5431 and
615 7263). It seems the least efficient is Case 2, although it is the one that, from a physical point of view,
616 is closest to reality. Nevertheless, each approach makes it possible to obtain satisfactory
617 representations.

618

619

620

621

622

623

624

625

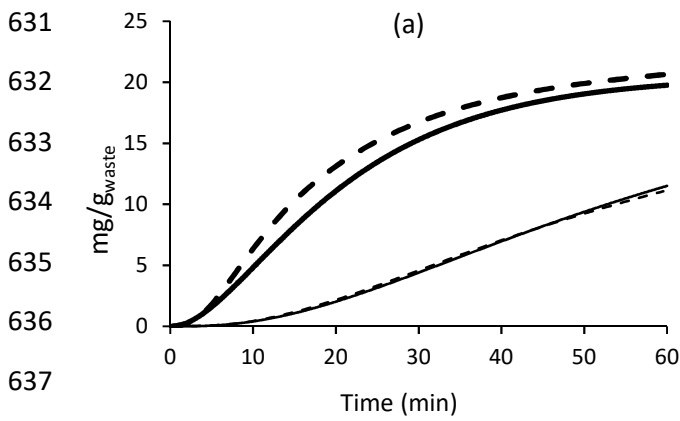
626

627

Table 6. The comparison of the different modeling approaches done by comparing the values of the sums of the error functions.

			erfc production flow						erfc cumulated masses					
			Case 1-a		Case 1-b		Case 2		Case 1-a		Case 1-b		Case 2	
			NH ₃	FA	NH ₃	FA	NH ₃	FA	NH ₃	FA	NH ₃	FA	NH ₃	FA
T°C	T(K)	SR	erfc dm _{NH₃}	erfc dm _{FA}	erfc dm _{NH₃}	erfc dm _{FA}	erfc dm _{NH₃}	erfc dm _{FA}	erfc m _{NH₃}	erfc m _{FA}	erfc m _{NH₃}	erfc m _{FA}	erfc m _{NH₃}	erfc m _{FA}
148	421	0.25	1.09	1.58	1.11	1.86	0.32	4.66	275.23	221.27	123.01	166.82	74.91	2463.83
148	421	0.5	0.55	1.30	0.68	1.18	0.07	0.99	137.99	310.08	256.14	187.66	8.07	160.91
148	421	0.75	0.06	2.39	0.06	2.40	0.08	0.86	2.94	392.44	5.73	373.93	10.18	66.33
Sum "Effect SR"			1.70	5.27	1.85	5.43	0.46	6.50	416.16	923.79	384.88	728.40	93.17	2691.07
139	412	0.75	0.21	5.43	0.20	5.46	0.10	2.64	25.99	1343.23	27.61	1374.95	23.32	1482.13
148	421	0.75	0.06	2.39	0.06	2.40	0.08	0.86	2.94	392.44	5.73	373.93	10.18	66.33
155.5	428.5	0.75	0.18	6.63	0.20	6.59	0.28	10.20	68.59	474.37	91.83	445.41	60.97	285.50
162	435	0.75	1.69	34.30	1.69	34.20	2.13	44.06	142.24	664.09	115.86	640.77	257.52	1039.01
168	441	0.75	1.60	49.52	1.64	49.55	1.87	41.11	91.82	698.40	121.19	684.67	37.82	883.04
Sum"Effect T"			3.74	98.27	3.78	98.20	4.46	98.86	331.58	3572.52	362.23	3519.72	389.83	3756.01
Sum (Effect SR and T)			5.44	103.54	5.63	103.63	4.93	105.36	747.73	4496.30	747.10	4248.12	483.00	6447.08
Global sum of error functions			108.98		109.26		110.29		5244.04		4995.23		6930.08	

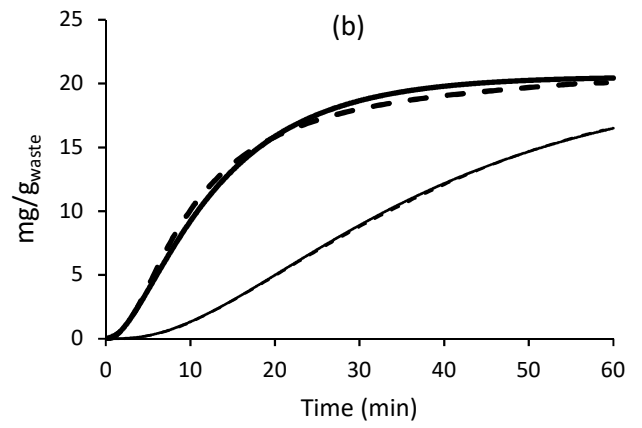
630



638

639

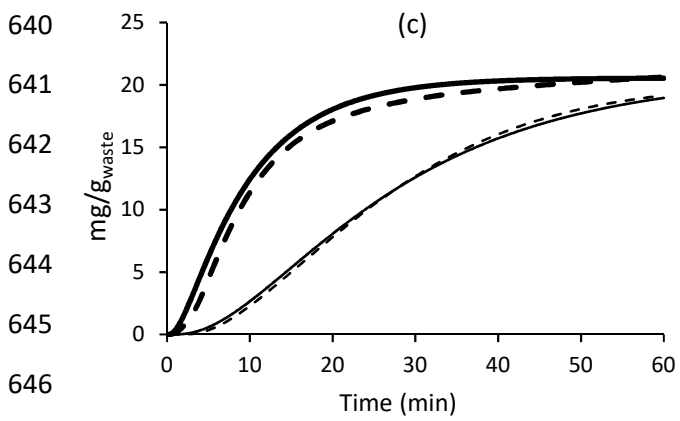
--- NH3_experimental — NH3_model
- - - FA_experimental — FA_model



647

648

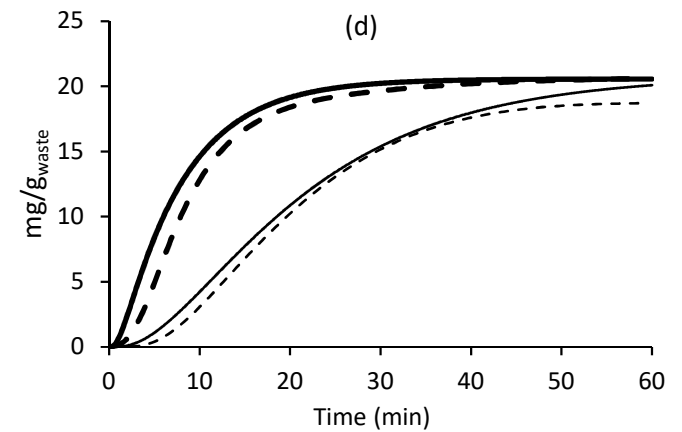
--- NH3_experimental — NH3_model
- - - FA_experimental — FA_model



657

658

--- NH3_experimental — NH3_model
- - - FA_experimental — FA_model



--- NH3_experimental — NH3_model
- - - FA_experimental — FA_model

659

660

661

662

663

664

665

666

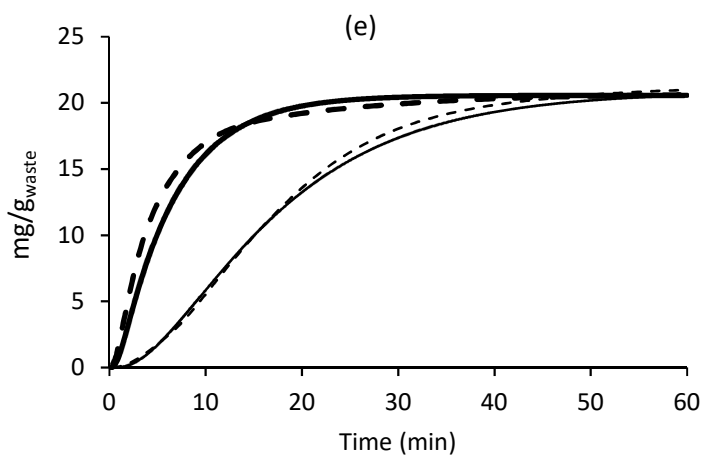
667

668

669

670

671



678

679

--- NH3_experimental — NH3_model
- - - FA_experimental — FA_model

Figure 11. Effect of steam ratio on cumulative masses of FA and NH₃ emitted from wood waste under (a) 2.5 bar, (b) 3.5 bar, (c) 4.5 bar, (d) 5.5 bar, and (e) 6.5 bar.

680

681

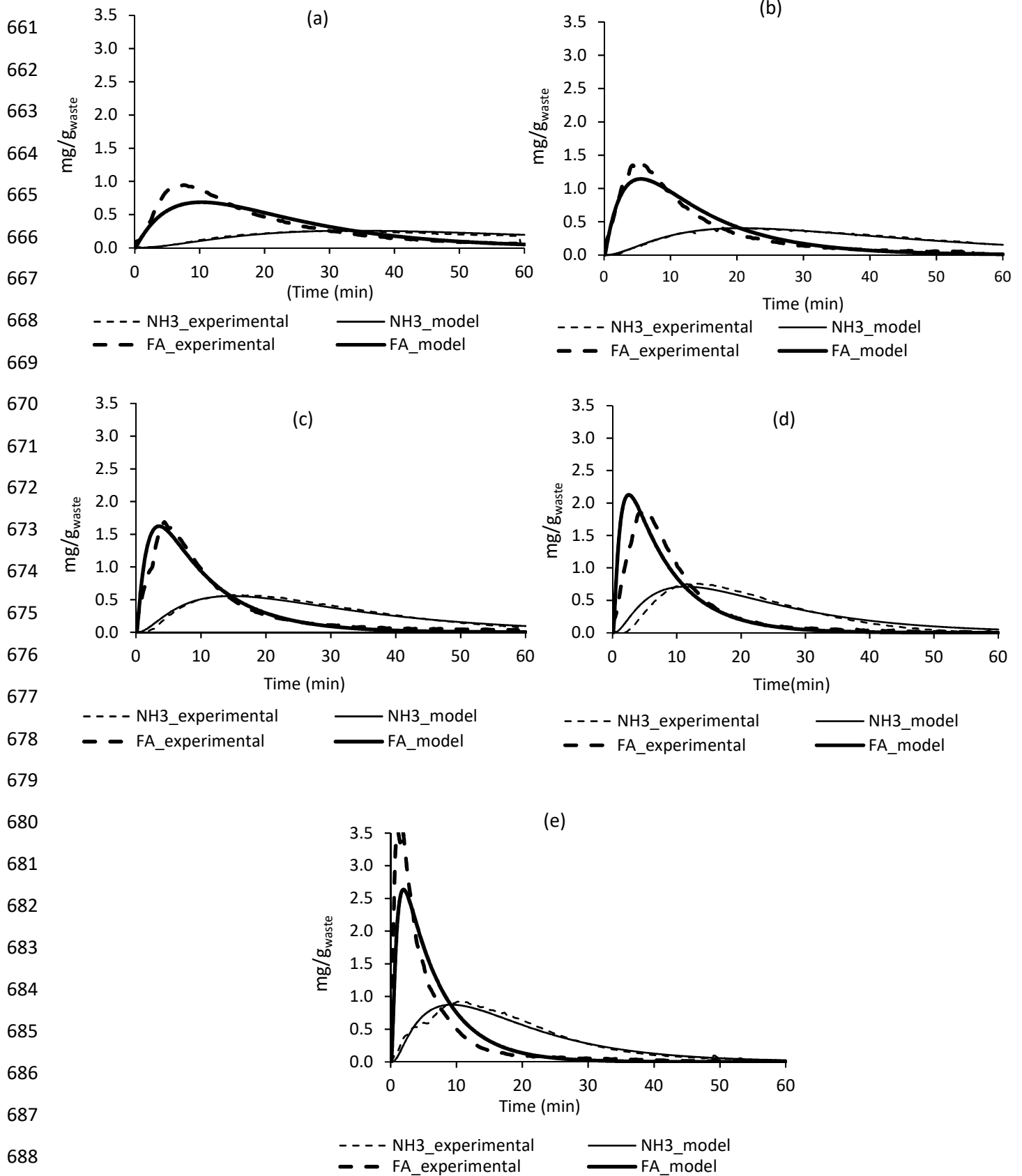
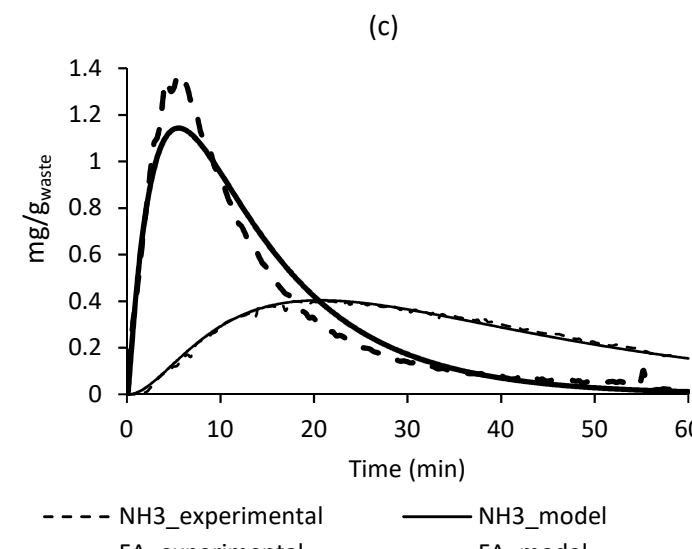
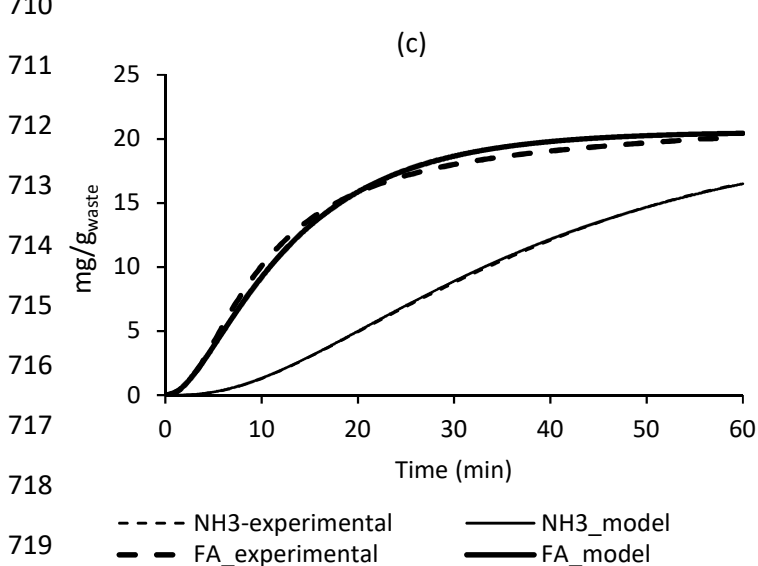
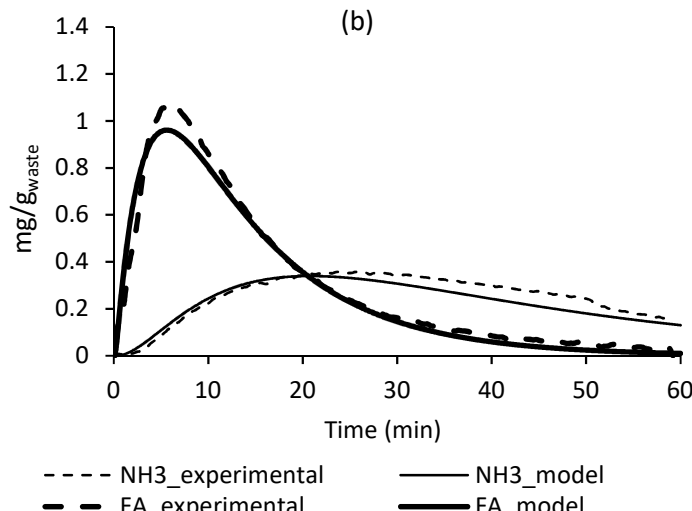
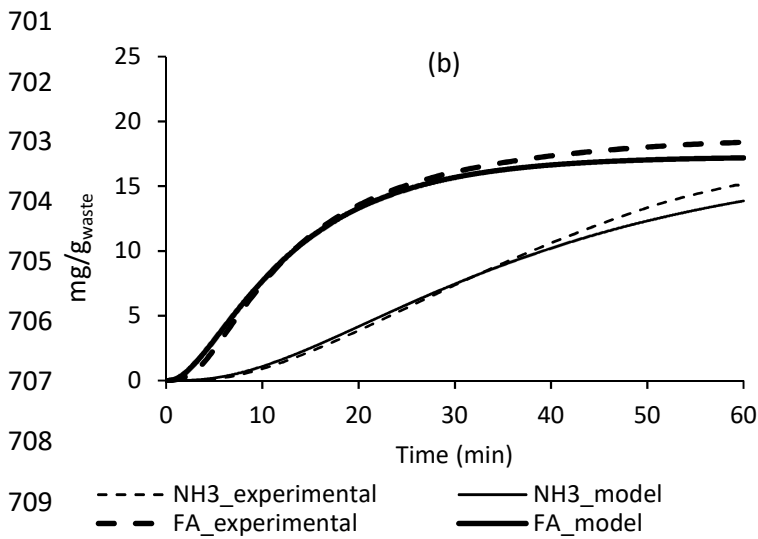
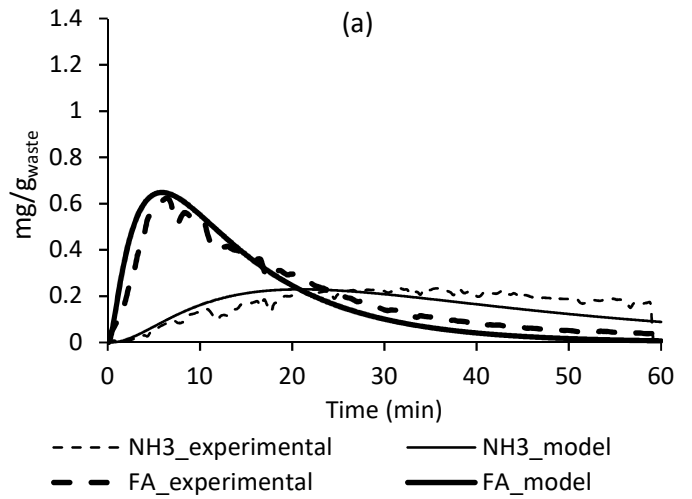
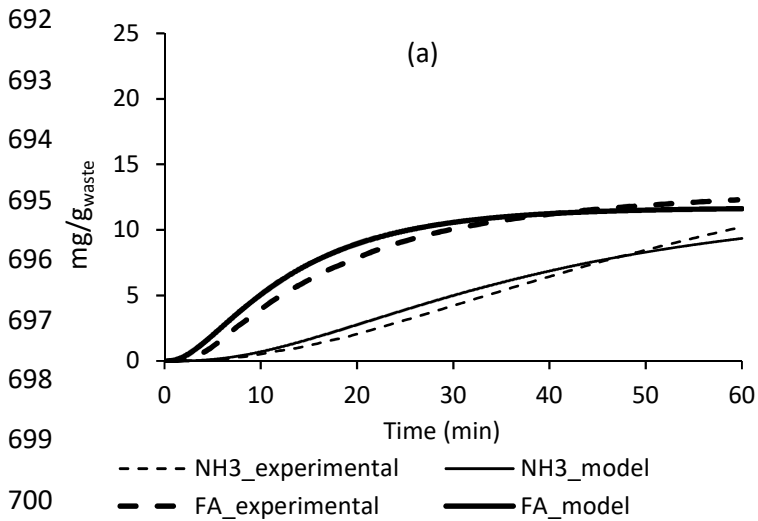


Figure 12. Effect of temperature on outlet flow of FA and NH₃ emission from wood waste under (a) 2.5 bar, (b) 3.5 bar, (c) 4.5 bar, (d) 5.5 bar, and (e) 6.5 bar.



720 Figure 13. Effect of steam ratio on cumulative masses of FA and NH₃
721 emitted from wood waste at steam ratio of (a) 0.25, (b) 0.5, and (c)
722 0.75 under 3.5 bar.

720 Figure 14. Effect of steam ratio on outlet flow of FA and NH₃ emission
721 from wood waste at steam ratio of (a) 0.25, (b) 0.5, and (c) 0.75 under
722 3.5 bar.

723 4. Conclusion

724 The effect of pressure/temperature and the steam ratio on the hydrolysis of wood waste has been
725 investigated. It could be first noticed that an original method to analyze gas emissions under rich
726 water vapor atmosphere by FTIR measurement has successfully been used.

727 The hydrolysis gas products were mainly formaldehyde and ammonia, while carbon dioxide was also
728 produced in low quantities. The evaluation of the effect of the steam ratio shows a dependence of
729 the quantity of formaldehyde and ammonia released below $1.5 \text{ g}_{\text{steam}}/\text{min}/\text{g}_{\text{waste}}$. A plateau is
730 observed for higher steam ratio values.

731 The evaluation of the effect of the pressure/temperature couple shows that total formaldehyde
732 emissions are independent of this factor. This point has not been experimentally demonstrated, but
733 the numerical model based on this assumption allows to well represent the experimental evolution
734 of ammonia.

735 The nitrogen removal rate in the range of 33 to 70% is reached, which shows the efficiency of the
736 hydrolysis process to remove resin from waste. Nitrogen balance shows a good correlation between
737 nitrogen elimination calculated from gas and solid analysis highlighting the reliability of the FTIR
738 measurement method, which also is confirmed by formaldehyde analysis using HPLC in the liquid
739 phase.

740 Finally, the three approaches proposed in this work for the numerical modelisation of ammonia and
741 formaldehyde emissions according to operatory conditions give all a good fitting between
742 experimental and calculated values. All information regarding quantification of ammonia and
743 formaldehyde emissions as well as numerical modelization could now be used as reliable technical
744 results to study the scale-up of such a process.

745

746 **Authors Contributions:** All authors have read and agree to the published version of the manuscript.
747 **Maximilien GIBIER:** Conceptualization, methodology, writing—original draft preparation
748 **Mohammad SADEGHISADEGHABAD:** Experimental work, formal analysis, writing—original draft
749 preparation **Pierre GIRODS:** methodology, formal analysis, numerical modelization, writing—original
750 draft preparation, writing—review and editing **André ZOULALIAN:** numerical modelization **Yann**
751 **ROGAUME:** Supervision, Funding acquisition

752 **Funding:** This research was funded by the Grand-Est region.

753 **Acknowledgments:** Authors wish to thank VALDELIA French Company for supplying the waste
754 material used in this work.

755 **Conflicts of interest:** The authors declare no conflicts of interest.

756

757

758 5. Reference

- 759 Bernstein, A., Sargent, E. H., Aspuru-Guzik, A., Cogdell, R., Fleming, G. R., Van Grondelle, R.,
760 & Molina, M. (2016). Renewables need a grand-challenge strategy. *Nature*,
761 538(7623), 30-30. <https://doi.org/10.1038/538030a>
- 762 Besserer, A., Troilo, S., Girods, P., Rogaume, Y., & Brosse, N. (2021). Cascading recycling of
763 wood waste: A review. *Polymers*, 13(11), 1752.
764 <https://doi.org/10.3390/polym13111752>
- 765 Cowling, E. B., & Merrill, W. (1966). Nitrogen in wood and its role in wood deterioration.
766 *Canadian Journal of Botany*, 44(11), 1539-1554. <https://doi.org/10.1139/b66-167>
- 767 Waste furniture sector France. (2020). Annual report of the Waste furniture sector in France.
768 [https://librairie.ademe.fr/dechets-economie-circulaire/1714-rapport-annuel-de-la-](https://librairie.ademe.fr/dechets-economie-circulaire/1714-rapport-annuel-de-la-filiere-des-dechets-d-elements-d-ameublement-dea-donnees-2018.html)
769 [filiere-des-dechets-d-elements-d-ameublement-dea-donnees-2018.html](https://librairie.ademe.fr/dechets-economie-circulaire/1714-rapport-annuel-de-la-filiere-des-dechets-d-elements-d-ameublement-dea-donnees-2018.html)
- 770 Girods, P. (2008). *Procédé multi-étagé de valorisation de déchets bois type panneaux de*
771 *particules* (Doctoral dissertation, Université Henri Poincaré-Nancy 1).
- 772 Girods, P., Dufour, A., Rogaume, Y., Rogaume, C., & Zoulalian, A. (2008). Thermal removal of
773 nitrogen species from wood waste containing urea formaldehyde and melamine
774 formaldehyde resins. *Journal of Hazardous Materials*, 159(2-3), 210-221.
775 <https://doi.org/10.1016/j.jhazmat.2008.02.003>
- 776 Girods, P., Dufour, A., Rogaume, Y., Rogaume, C., & Zoulalian, A. (2009a). Comparison of
777 gasification and pyrolysis of thermal pre-treated wood board waste. *Journal of*
778 *Analytical and Applied Pyrolysis*, 85(1-2), 171-183.
779 <https://doi.org/10.1016/j.jaap.2008.11.014>
- 780 Girods, P., Dufour, A., Fierro, V., Rogaume, Y., Rogaume, C., Zoulalian, A., & Celzard, A.
781 (2009b). Activated carbons prepared from wood particleboard wastes:
782 Characterisation and phenol adsorption capacities. *Journal of Hazardous Materials*,
783 166(1), 491-501. <https://doi.org/10.1016/j.jhazmat.2008.11.047>
- 784 Grigsby, W. J., Thumm, A., Carpenter, J. E., & Hati, N. (2014). Investigating the extent of urea
785 formaldehyde resin cure in medium density fibreboard: Characterisation of
786 extractable resin components. *International Journal of Adhesion and Adhesives*, 50,
787 50-56. <https://doi.org/10.1016/j.ijadhadh.2013.12.020>
- 788 Hagel, S., & Saake, B. (2020). Fractionation of waste MDF by steam refining. *Molecules*,
789 25(9), 2165. <https://doi.org/10.3390/molecules25092165>
- 790 Hepburn, J. S. (1908). The modifications of the Kjeldahl method for the quantitative
791 determination of nitrogen. *Journal of the Franklin Institute*, 166(2), 81-99.
792 [https://doi.org/10.1016/S0016-0032\(08\)90028-4](https://doi.org/10.1016/S0016-0032(08)90028-4)
- 793 Ihnát, V., Lübke, H., Russ, A., & Borůvka, V. (2017). Waste agglomerated wood materials as a
794 secondary raw material for chipboards and fibreboards Part I. Preparation and
795 characterization of wood chips in terms of their reuse. *Wood research*, 62(1), 45-56.
- 796 Irle, M., Barbu, M., Thoeman, H., Inggris, G. B., Irle, M., & Sernek, M. (2010). Wood based
797 panels: an introduction for specialists. *Wood-based Panel Technology*, Cost Action
798 E49, 1.
- 799 Jiang, X., Li, C., Chi, Y., & Yan, J. (2010). TG-FTIR study on urea-formaldehyde resin residue
800 during pyrolysis and combustion. *Journal of Hazardous Materials*, 173(1-3), 205-210.
801 <https://doi.org/10.1016/j.jhazmat.2009.08.070>

802 Kraft, R., & Roffael, E. (2003). Thermohydrolytischer abbau von mitteldichten faserplatten.
803 *adhäsion KLEBEN & DICHTEN*, 47(10), 38-41. <https://doi.org/10.1007/BF03244013>

804 Lee, M., Prewitt, L., & Mun, S. P. (2014). Formaldehyde release from medium density
805 fiberboard in simulated landfills for recycling. *Journal of the Korean Wood Science*
806 *and Technology*, 42(5), 597-604. <https://doi.org/10.5658/WOOD.2014.42.5.597>

807 Li, J., Zhu, J., & Ye, L. (2007). Determination of formaldehyde in squid by high-performance
808 liquid chromatography. *Asia Pac. J. Clin. Nutr*, 16(1), 127-130.

809 L Liu, M., Wang, Y., Wu, Y., & Wan, H. (2018). Hydrolysis and recycling of urea formaldehyde
810 resin residues. *Journal of Hazardous Materials*, 355, 96-103..
811 <https://doi.org/10.1016/j.jhazmat.2018.05.019>

812 Lubis, M. A. R., Hong, M. K., & Park, B. D. (2018). Hydrolytic removal of cured urea-
813 formaldehyde resins in medium-density fiberboard for recycling. *Journal of Wood*
814 *Chemistry and Technology*, 38(1), 1-14.
815 <https://doi.org/10.1080/02773813.2017.1316741>

816 Lubis, M. A. R., & Park, B. D. (2018). Analysis of the hydrolysates from cured and uncured
817 urea-formaldehyde (UF) resins with two F/U mole ratios. *Holzforschung*, 72(9), 759-
818 768. <https://doi.org/10.1515/hf-2018-0010>.

819 Lubis, M. A. R., Hidayat, W., Zaini, L. H., & Park, B. D. (2020). Effects of Hydrolysis on the
820 Removal of Cured Urea-Formaldehyde Adhesive in Waste Medium-Density
821 Fiberboard. *Jurnal Sylva Lestari*, 8(1), 1-9. <https://doi.org/10.23960/jsl181-9>

822 Lubis, M. A. R., Manohar, S. Y., Laksana, R. P. B., Fatriasari, W., Ismayati, M., Falah, F., ... &
823 Hidayat, W. (2021). The Removal of Cured Urea-Formaldehyde Adhesive Towards
824 Sustainable Medium Density Fiberboard Production: A Review. *Jurnal Sylva Lestari*,
825 9(1), 23-44. <https://doi.org/10.23960/jsl1923-44>.

826 Lubke, H., Ihnát, V., Kuňa, V., & Balberčák, J. (2020). A multi-stage cascade use of wood
827 composite boards. *Wood Res*, 65, 843-854.

828 Lykidis, C., & Grigoriou, A. (2008). Hydrothermal recycling of waste and performance of the
829 recycled wooden particleboards. *Waste Management*, 28(1), 57-63.
830 <https://doi.org/10.1016/j.wasman.2006.11.016>

831 Myers, G.E., (1986). Mechanisms of Formaldehyde Release from Bonded Wood Products, in:
832 Formaldehyde Release from Wood Products, ACS Symposium Series. American
833 Chemical Society, pp. 87–106. <https://doi.org/10.1021/bk-1986-0316.ch008>.

834 Myers, G.E., (1982). Hydrolytic stability of cured urea-formaldehyde resins. *Journal of Wood*
835 *Science*, 2, 127–138

836 Myers, G. E., & Koutsky, J. A. (1990). Formaldehyde Liberation and Cure Behavior of Urea-
837 Formaldehyde Resins. *Holzforschung*, 44(2), 117-126.
838 <https://doi.org/10.1515/hfsg.1990.44.2.117>

839 Nishikawa, H., & Sakai, T. (1995). Derivatization and chromatographic determination of
840 aldehydes in gaseous and air samples. *Journal of Chromatography A*, 710(1), 159-165.
841 [https://doi.org/10.1016/0021-9673\(94\)01006-Z](https://doi.org/10.1016/0021-9673(94)01006-Z)

842 Park, B. D., & Causin, V. (2013). Crystallinity and domain size of cured urea-formaldehyde
843 resin adhesives with different formaldehyde/urea mole ratios. *European Polymer*
844 *Journal*, 49(2), 532-537. <https://doi.org/10.1016/j.eurpolymj.2012.10.029>

845 Park, B. D., & Jeong, H. W. (2011). Hydrolytic stability and crystallinity of cured urea-
846 formaldehyde resin adhesives with different formaldehyde/urea mole ratios.

847 *International Journal of Adhesion and Adhesives*, 31(6), 524-529.
848 <https://doi.org/10.1016/j.ijadhadh.2011.05.001>

849 Park, B. D., & Lee, S. M. (2015). Hydrolytic Stability of Cured Urea-Melamine-Formaldehyde
850 Resins Depending on Hydrolysis Conditions and Hardener Types. *Journal of the*
851 *Korean Wood Science and Technology*, 43(5), 672-681.
852 <https://doi.org/10.5658/WOOD.2015.43.5.672>

853 Pizzi, A. and Mittal, K. L., eds. (2003). *Handbook of Adhesive Technology*, 2nd edn, New York,
854 NY: Marcel Dekker. <https://doi.org/10.1201/9780203912225>

855 Ren, T., Wang, Y., Wu, N., Qing, Y., Li, X., Wu, Y., & Liu, M. (2022). Degradation of urea-
856 formaldehyde resin residues by a hydrothermal oxidation method into recyclable
857 small molecular organics. *Journal of Hazardous Materials*, 426, 127783.
858 <https://doi.org/10.1016/j.jhazmat.2021.127783>

859 Ringena, O., Janzon, R., Pfizenmayer, G., Schulte, M., & Lehnen, R. (2006). Estimating the
860 hydrolytic durability of cured wood adhesives by measuring formaldehyde liberation
861 and structural stability. *Holz als Roh-und werkstoff*, 64(4), 321-326.
862 <https://doi.org/10.1007/s00107-005-0087-3>

863 Samaržija-Jovanović, S., Jovanović, V., Konstantinović, S., Marković, G., & Marinović-Cincović,
864 M. (2011). Thermal behavior of modified urea-formaldehyde resins. *Journal of*
865 *thermal analysis and calorimetry*, 104(3), 1159-1166.
866 <https://doi.org/10.1007/s10973-010-1143-8>

867 Wahed, P., Razzaq, M. A., Dharmapuri, S., & Corrales, M. (2016). Determination of
868 formaldehyde in food and feed by an in-house validated HPLC method. *Food*
869 *chemistry*, 202, 476-483. <https://doi.org/10.1016/j.foodchem.2016.01.136>

870 Wan, H., Wang, X. M., & Shen, J. (2014). Recycling wood composite panels: Characterizing
871 recycled materials. *BioResources*, 9(4), 7554-7565.

872 Xu, X., Su, R., Zhao, X., Liu, Z., Li, D., Li, X., ... & Wang, Z. (2011). Determination of
873 formaldehyde in beverages using microwave-assisted derivatization and ionic liquid-
874 based dispersive liquid-liquid microextraction followed by high-performance liquid
875 chromatography. *Talanta*, 85(5), 2632-2638.
876 <https://doi.org/10.1016/j.talanta.2011.08.037>

877

